Nonadiabatic Variational Gaussian Wavepacket Dynamics: Interpolating between Accurate Quantum Dynamics and the Quantum-Classical Limit

I. Burghardt

Institute for Physical and Theoretical Chemistry, Goethe University Frankfurt, Germany

CECAM Workshop
"Non-Adiabatic Quantum Dynamics: From Theory To Experiments"
Lausanne, 2-6 July, 2018

Acknowledgments

- M. Ruckenbauer, S. Römer (group Frankfurt)
- P. Eisenbrandt, M. Bonfanti (group Frankfurt)
- T. Ma, R. Hegger (group Frankfurt)
- B. Kloss (group Frankfurt, now Columbia University)
- C. Lubich (Tübingen, Germany)
- E. Pollak, J. Petersen (Weizmann Institute, Israel)
- D. Tannor, W. Koch (Weizmann Institute, Israel)
- B. Poirier (Texas Tech, USA)
- G. A. Worth (UCL London, UK)
- J. C. Tremblay (FU Berlin, Germany)
- D. Shalashilin (Leeds, UK)
- R. Martinazzo (Milano, Italy)

Topics

1. Gaussian-based MCTDH (G-MCTDH)
   - Preamble: Time-Dependent Variational Principle & MCTDH
   - Multi-Layer MCTDH
   - Quantum-Semiclassical MCTDH: G-MCTDH, vMCG

Topics

1. Gaussian-based MCTDH (G-MCTDH)
   - Preamble: Time-Dependent Variational Principle & MCTDH
   - Multi-Layer MCTDH
   - Quantum-Semiclassical MCTDH: G-MCTDH, vMCG
2. Two-Layer/Multi-Layer G-MCTDH
   - Two-Layer Extension – Concept
   - Equations of Motion
   - Applications: Donor-Acceptor System

Topics

1. Gaussian-based MCTDH (G-MCTDH)
   - Preamble: Time-Dependent Variational Principle & MCTDH
   - Multi-Layer MCTDH
   - Quantum-Semiclassical MCTDH: G-MCTDH, vMCG
2. Two-Layer/Multi-Layer G-MCTDH
   - Two-Layer Extension – Concept
   - Equations of Motion
   - Applications: Donor-Acceptor System
3. Quantum-Classical Limit of G-MCTDH
   - Semiclassically Scaled G-MCTDH
   - Quantum-Classical Dynamics
   - Variational Multiconfigurational Ehrenfest Dynamics

Approximate Wavefunctions from the Dirac-Frenkel Variational Principle

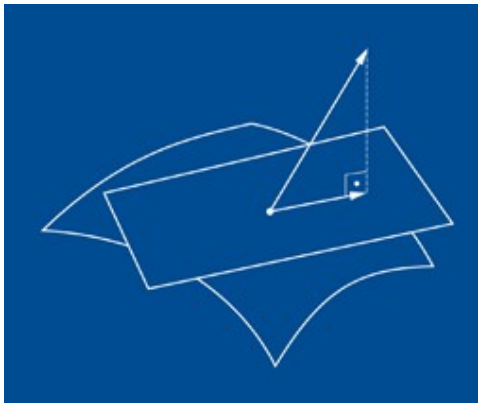

C. Lubich, From Quantum to Classical Molecular Dynamics: Reduced Models and Numerical Analysis, Zürich (2008)

Dirac-Frenkel variational principle (DFVP):

$\langle \delta\Psi | \hat{H} - i\frac{\partial}{\partial t} | \Psi \rangle = 0 \quad \longrightarrow$ dynamical equation for $\dot{\Psi}$

where $\delta\Psi \in \mathscr{T}_\Psi \mathscr{M}$ (tangent space wrt the approximate manifold $\mathscr{M}$ on which the wavefunction is defined)

Dirac 1930, Frenkel 1934, McLachlan 1964

- the time derivative is then given by
  $\dot{\Psi} = \mathscr{P}(\Psi)\frac{1}{i}\hat{H}\Psi$
  where $\mathscr{P}(\Psi)$ projects onto the tangent space
- the residual is minimized: $||\dot{\Psi} - \frac{1}{i}\hat{H}\Psi|| = \min$
- interpretation as action principle:
  $\delta S(\Psi) = \delta \int_{t_0}^{t_1} \langle \Psi(t) | i\frac{\partial}{\partial t} - \hat{H} | \Psi(t) \rangle dt = 0$
- symplectic flow: norm and energy conservation

Unitary Dynamics in Many Dimensions: MCTDH

$$\Psi(r,t) = \sum_J A_J(t)\ \Phi_J(r,t) \equiv \sum_{j_1=1}^{n_1} \dots \sum_{j_f=1}^{n_f} A_{j_1 \dots j_f}(t) \prod_\kappa \varphi_{j_\kappa}^{(\kappa)}(r_\kappa,t)$$

- Multi-Configuration Time-Dependent Hartree
  Meyer, Manthe, Cederbaum, Chem. Phys. Lett. **165**, 73 (1990), Beck et al., Phys. Rep. **324**, 1 (2000)
- EoM's from the Dirac-Frenkel variational principle: $\langle \delta\Psi | \hat{H} - i\frac{\partial}{\partial t} | \Psi \rangle = 0$
- MCTDH takes one to 50-100 modes; exponential scaling alleviated
- restriction on the form of the potential: sums over products

- related multi-layer variant (ML-MCTDH) goes up to 1000 modes
  Wang, Thoss, J. Chem. Phys. 119, 1289 (2003), Manthe, J. Chem. Phys. 128, 164116 (2008), Vendrell, Meyer, *ibid* 134, 044135 (2011)
- related MCTDH-F (fermion) and MCTDH-B (boson) methods
  Kato, Kono, Chem. Phys. Lett. 392, 533 (2004), Nest, Klamroth, Saalfrank, J. Chem. Phys. 122, 124102 (2005)
  Alon, Streltsov, Cederbaum, Phys. Lett. A 362, 453 (2007)
- density matrix variant
  Raab, Burghardt, Meyer, J. Chem. Phys. 111, 8759 (1999)
- hybrid approaches: e.g., Gaussian-based variant (G-MCTDH, vMCG)
  Burghardt, Meyer, Cederbaum, J. Chem. Phys. 111, 2927 (1999), Worth, Burghardt, Chem. Phys. Lett. 368, 502 (2003)

Unitary Dynamics in Many Dimensions: MCTDH

MCTDH: optimal, compact time-dependent SPF basis

Meyer, Manthe, Cederbaum, Chem. Phys. Lett. **165**, 73 (1990), Beck et al., Phys. Rep. **324**, 1 (2000)

$$\Psi(r,t) = \sum_J A_J(t)\ \Phi_J(r,t)$$

$$= \sum_{j_1=1}^{n_1} \dots \sum_{j_f=1}^{n_f} A_{j_1 \dots j_N}(t)\, \varphi_{j_1}^{(1)}(r_1,t) \dots \varphi_{j_f}^{(f)}(r_f,t)$$

A_J: coefficient vector

Φ_J: configurations

$\varphi_{j_\kappa}^{(\kappa)}$: single-particle functions (SPFs) – to be represented in a primitive basis $\{\chi_{i_\kappa}\}$

Another convenient notation:

$$\Psi(r,t) = \sum_{j_\kappa=1}^{n_\kappa} \varphi_{j_\kappa}^{(\kappa)}(r_\kappa,t)\, \psi_{j_\kappa}^{(\kappa)}(r_1,\dots,r_{\kappa-1},r_{\kappa+1},\dots,r_N,t)$$

$\psi_{j_\kappa}^{(\kappa)}$: single-hole functions (SHFs) $\longrightarrow$ $\rho_{ij}^{(\kappa)} = \langle \psi_j^{(\kappa)} | \psi_i^{(\kappa)} \rangle$ reduced density

MCTDH as Low-Rank Tensor Approximation Scheme

MCTDH: Tucker format representation of coefficient tensor

Consider $\Psi(r,t)$ in terms of the primitive basis (typically DVR[1] grid):

$$\Psi(r,t) = \sum_{i_1=1}^{N_1} \cdots \sum_{i_f=1}^{N_f} Y_{i_1 \ldots i_f}(t) \prod_{\kappa=1}^{f} \chi_{i_\kappa}^{(\kappa)}(r_\kappa)$$

Tucker format of the coefficient tensor $Y_{i_1 \ldots i_f}(t)$:

$$Y_{i_1 \ldots i_f}(t) = \sum_{j_1=1}^{n_1} \cdots \sum_{j_f=1}^{n_f} A_{j_1 \ldots j_f}(t) \prod_{\kappa=1}^{f} U_{i_\kappa j_\kappa}^{(\kappa)}(t)$$

noting that $n_\kappa \ll N_\kappa$

A_J: core tensor

$U_{i_\kappa j_\kappa}^{(\kappa)} = \langle \chi_{i_\kappa}^{(\kappa)} | \varphi_{j_\kappa}^{(\kappa)} \rangle$ representation of SPFs in the primitive basis

$\varphi_{j_\kappa}^{(\kappa)}$: single-particle functions (SPFs)

$\chi_{i_\kappa}^{(\kappa)}$: primitive basis functions

[1] DVR = Discrete Variable Representation

Bachmayr, Schneider, Uschmajew, Found. Comp. Math. 16, 1423 (2016)

MCTDH – Equations of Motion

Coupled system of coefficient equations and low-dimensional non-linear equations for single-particle functions (SPFs) $\varphi^{(\kappa)}$:

coefficients:
$$i\frac{dA_J}{dt} = \sum_L \langle \Phi_J | H | \Phi_L \rangle A_L$$

SPFs:
$$i\frac{\partial \varphi^{(\kappa)}}{\partial t} = \left(\hat{1} - \hat{P}^{(\kappa)}\right)\left[\rho^{(\kappa)}\right]^{-1} \hat{H}^{(\kappa)} \varphi^{(\kappa)}$$

Meyer, Manthe, Cederbaum, CPL **165**, 73 (1990), Beck et al., Phys. Rep. **324**, 1 (2000)

- $\hat{P}^{(\kappa)} = \sum_j |\varphi_j^{(\kappa)}\rangle\langle\varphi_j^{(\kappa)}|$ is the time-dependent projector on the κth subspace
- $\hat{H}_{ij}^{(\kappa)} = \langle \psi_i^{(\kappa)} | \hat{H} | \psi_j^{(\kappa)} \rangle$ are mean-field Hamiltonian matrix elements
- $\rho_{ij}^{(\kappa)} = \langle \psi_i^{(\kappa)} | \psi_j^{(\kappa)} \rangle$ are reduced density matrix elements in the κth subspace
- recent approaches to "repair" singularity problem ($[\rho^{(\kappa)}]^{-1}$)

Manthe, J. Chem. Phys. **142**, 244109 (2015), Wang, Meier, J. Chem. Phys. **148**, 124105 (2018),
Lubich, Appl. Math. Res. Express 2, 311-328 (2015), Kloss, Burghardt, Lubich. J. Chem. Phys., 146, 174107 (2017)

Derivation of MCTDH Equations of Motion: Two Procedures

- standard procedure: construct explicit form of wavefunction variation:

$$\delta\Psi = \sum_J \delta A_J \, \Phi_J + \sum_\kappa \left(\sum_{l_\kappa} \delta\varphi_{l_\kappa}^{(\kappa)} \Psi_{l_\kappa}^{(\kappa)} \right)$$

and insert independent variations δA_J and $\delta\varphi_{l_\kappa}^{(\kappa)}$ into the DFVP:

$$\langle \delta\Psi | \hat{H} - i\frac{\partial}{\partial t} | \Psi \rangle = 0$$

- alternative procedure: obtain tangent-space projector

$$\mathscr{P}(\Psi) = \mathscr{P}_0(\Psi) + \sum_\kappa \mathscr{P}_\kappa(\Psi)$$

and insert component projectors into the projected TDSE:

$$i\frac{\partial}{\partial t} | \Psi \rangle = \mathscr{P}(\Psi) \hat{H} | \Psi \rangle$$

C. Lubich, From Quantum to Classical Molecular Dynamics: Reduced Models and Numerical Analysis, Zürich (2008)

Tangent Space Projector for MCTDH

$$\mathscr{P}(\Psi) = \mathscr{P}_0(\Psi) + \sum_\kappa \mathscr{P}_\kappa(\Psi)$$

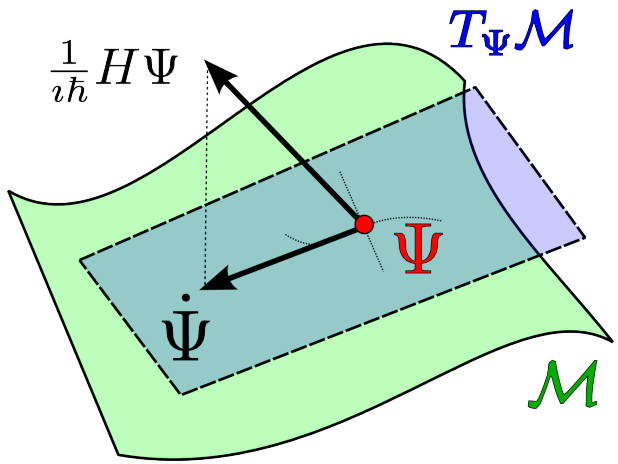

$$\mathscr{P}_0(\Psi) = \sum_J |\Phi_J\rangle\langle\Phi_J| \quad \text{and} \quad \mathscr{P}_\kappa(\Psi) = \left(1 - P^{(\kappa)}\right) \otimes \bar{P}^{(\kappa)}$$

$P^{(\kappa)} = \sum_i |\varphi_i^{(\kappa)}\rangle\langle\varphi_i^{(\kappa)}|$: SPF subspace projector

$\bar{P}^{(\kappa)} = \sum_{l,l'} |\Psi_l^{(\kappa)}\rangle (\rho^{(\kappa)})^{-1}_{l'l} \langle\Psi_{l'}^{(\kappa)}|$: SHF projector (noting non-orthogonality!)

Koch, Lubich, SIAM J. Matrix Anal. Appl. 31, 2360 (2010), Kloss, Burghardt, Lubich. J. Chem. Phys., 146, 174107 (2017)
Bonfanti, Burghardt, Chem. Phys., in press (2018), arXiv:1802.01058 [physics.chem-ph]

Advantage of using this route: new concepts of how to split $\mathscr{P}$

Multi-Layer Form

$$\Psi(t) = \sum_J A_J^{[1]}(t)\Phi_J^{[1]}(t) := \sum_J A_J^{[1]}(t) \prod_{\kappa_1=1}^{f^{[1]}} \varphi_{j_{\kappa_1}}^{[1](\kappa_1)}(t)$$

with the spf's of the first $M-1$ layers ($m \in \{2,3,\ldots,M\}$),

$$\varphi_j^{[m-1](\mu_m-1)}(t) \quad = \quad \sum_J A_{j,J}^{[m](\mu_m-1)}(t)\Phi_J^{[m](\mu_m-1)}(t) = \sum_J A_{j,J}^{[m](\mu_m-1)}(t) \prod_{\kappa_m=1}^{f_{\mu_{m-1}}^{[m]}} \varphi_{j_{\kappa_m}}^{[m]}(t)$$

and the final (Mth) layer particles are expressed in the primitive basis,

$$\varphi_j^{[M](\mu_M)}(r_{\mu_M},t) = \sum_l U_{jl}^{[M](\mu_M)}(t)\chi_l(r_{\mu_M})$$

- hierarchical Tucker format

Wang, Thoss, J. Chem. Phys. 119, 1289 (2003), Manthe, J. Chem. Phys. 128, 164116 (2008), Vendrell, Meyer, *ibid* 134, 044135 (2011)

Quantum Dynamics: Hierarchical Multi-Layer MCTDH Tree

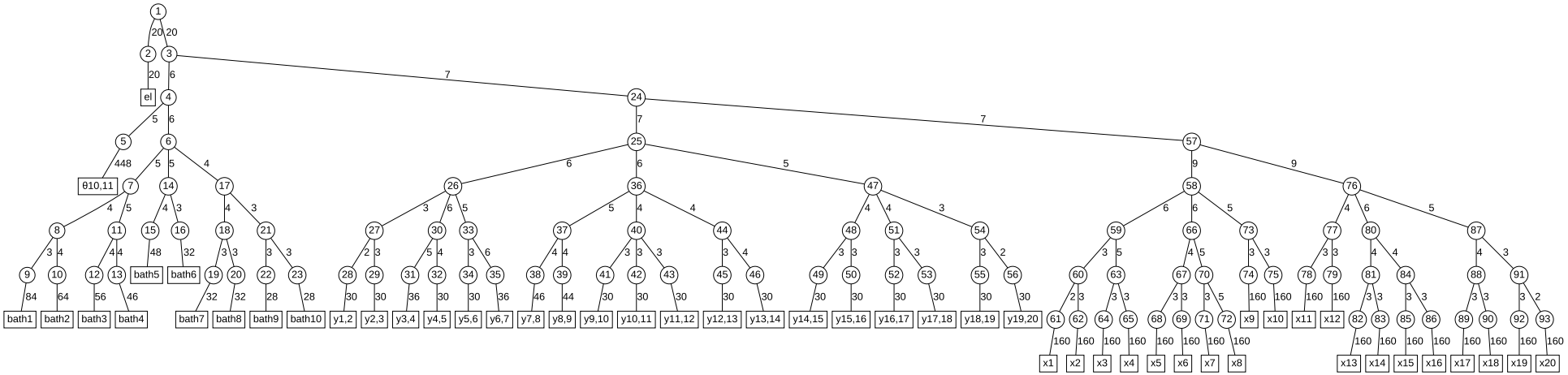

- ML-MCTDH (20 states, 50 modes)
- 7 layers, 2-10 single-particle functions (SPFs) – highly correlated system!
- combined electronic particle (here, 20 states)
- active torsional mode as isolated particle (long DVR grid)
- delocalized initial condition prepared by imaginary time propagation

Binder, Lauvergnat, Burghardt, Phys. Rev. Lett. 120, 227401 (2018), Supp. Mater.

Exciton Dynamics in an Oligothiophene OT-20 Segment

- Do we see trapped exciton-polarons in the dynamics?
- How exactly does the exciton migrate as the conjugation break "heals"?
- How does the spatial extension of the exciton change as a function of conformational (torsional) fluctuations?

Monomer representation:
most unbiased picture to answer these questions!

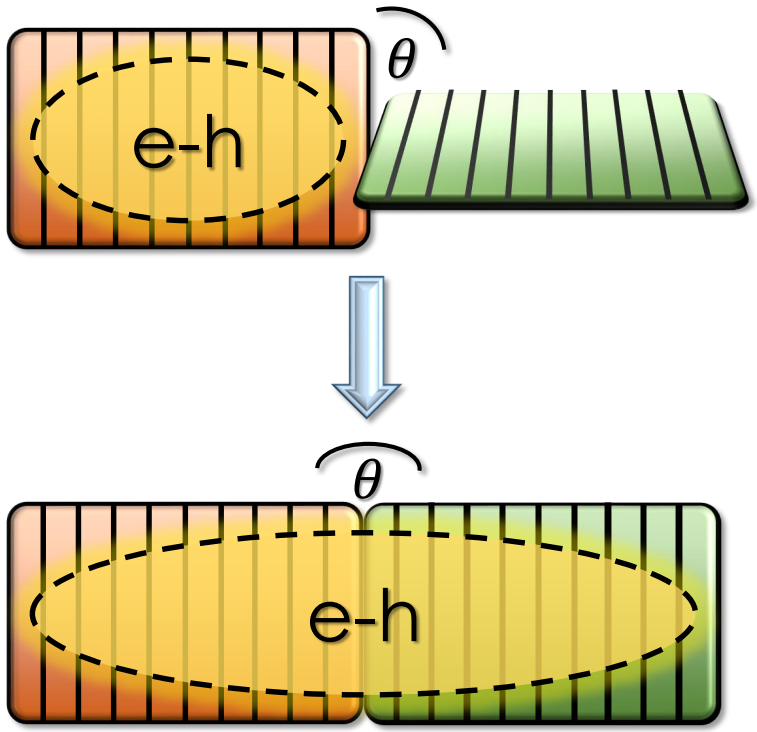

Quantum Dynamics: 20-Site J-Aggregate with Central Torsion

C-C inter-monomer mode + local C=C + torsion + bath

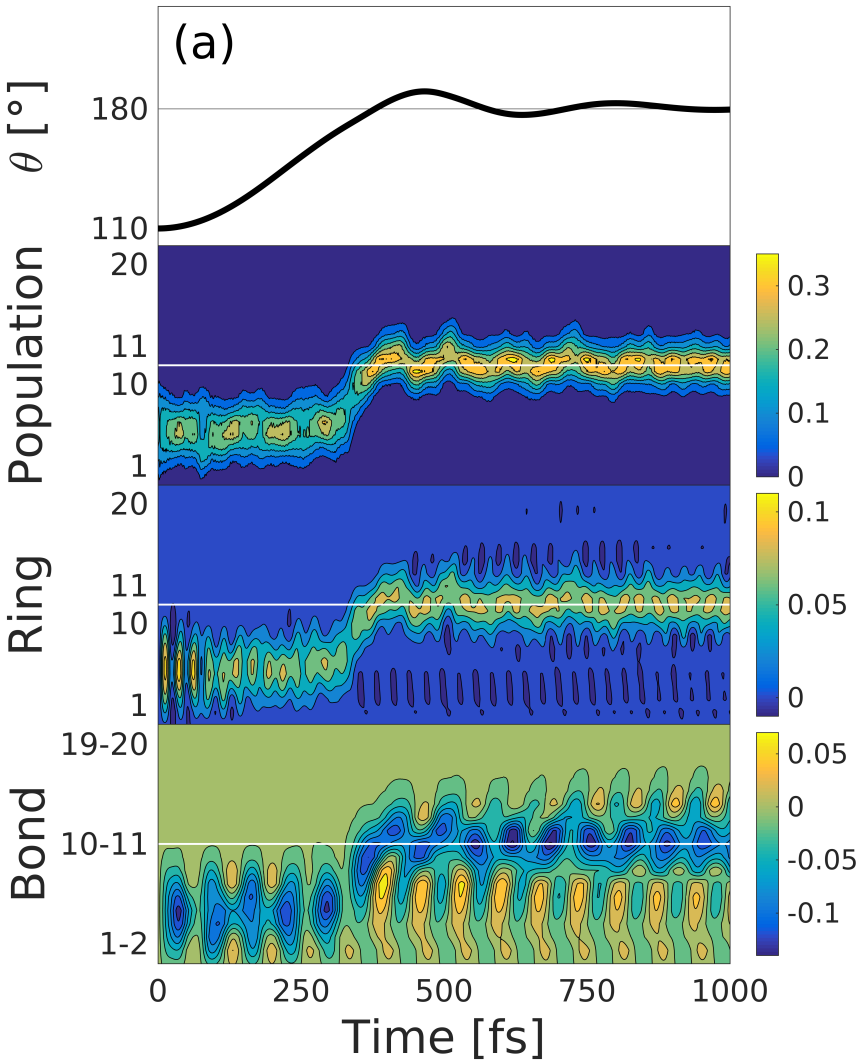

C-C inter-monomer + torsion + bath

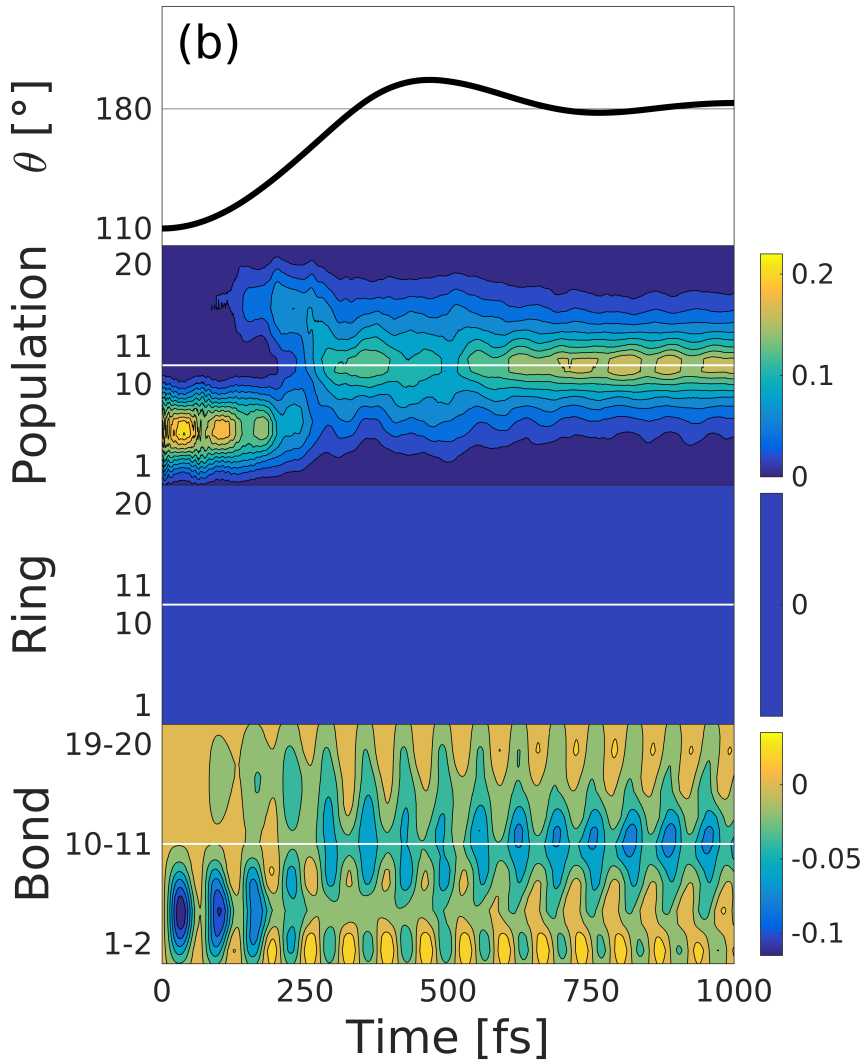

Semiclassical SQC/MM dynamics (T=0K)

SQC/MM – single trajectory

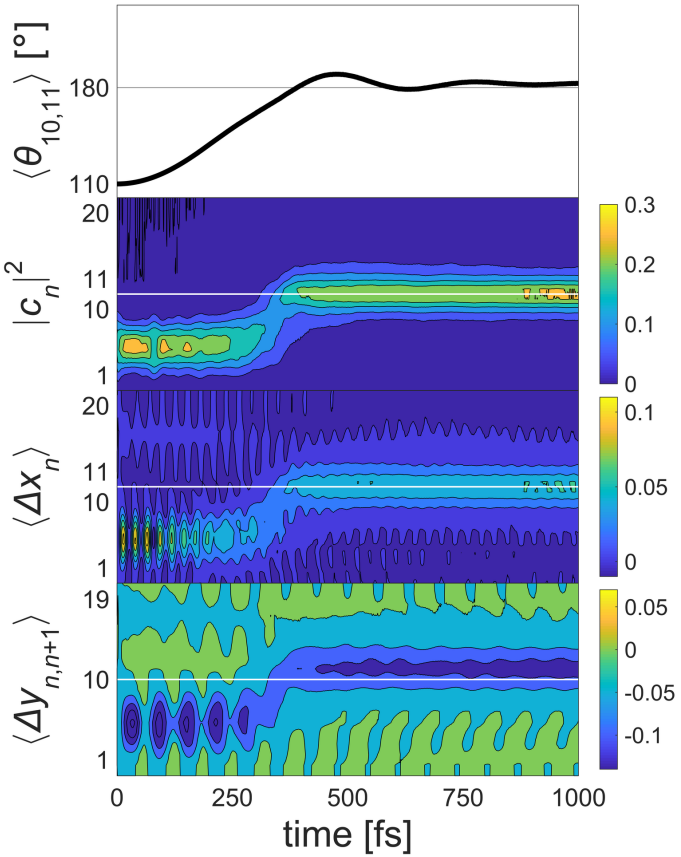

SQC/MM – Wigner average

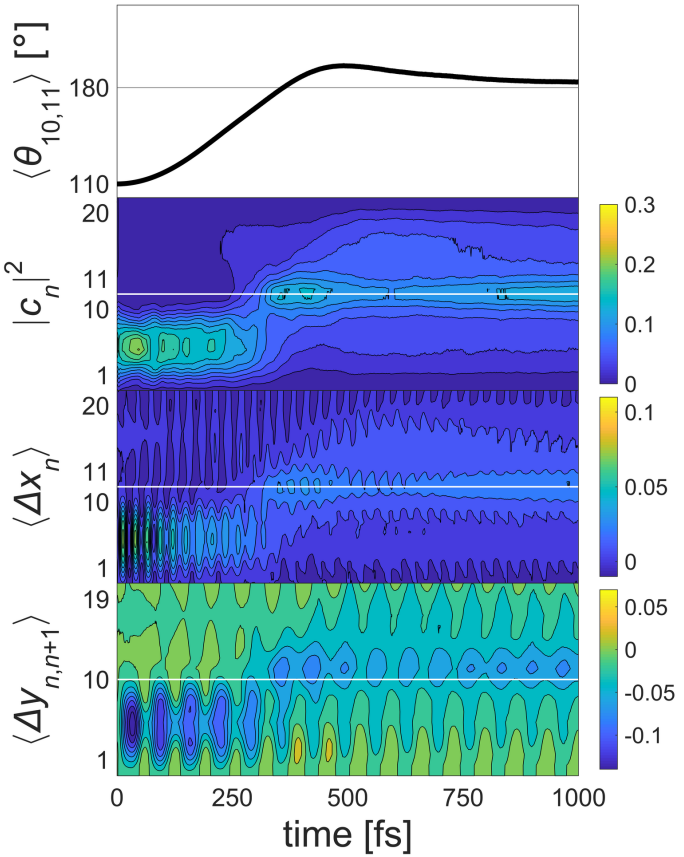

- SQC/MM = Symmetrical Quasi-Classical / Meyer-Miller model
- single-trajectory result close to MCTDH, but Wigner average "fuzzy"

Liang, Cotton, Binder, Hegger, Burghardt, Miller, J. Chem. Phys., in press (2018)

Gaussian-based MCTDH (G-MCTDH)

Burghardt, Meyer, Cederbaum, J. Chem. Phys. 111, 2927 (1999)

$$\Psi(r,t) = \sum_J A_J(t)\Phi_J(r,t) \quad ; \quad \Phi_J(r,t) = \underbrace{\prod_{\kappa=1}^{M} \varphi_{j_\kappa}^{(\kappa)}(r_\kappa,t)}_{\text{SPFs}} \underbrace{\prod_{\kappa=M+1}^{P} g_{j_\kappa}^{(\kappa)}(r_\kappa,t)}_{\text{GWPs}}$$

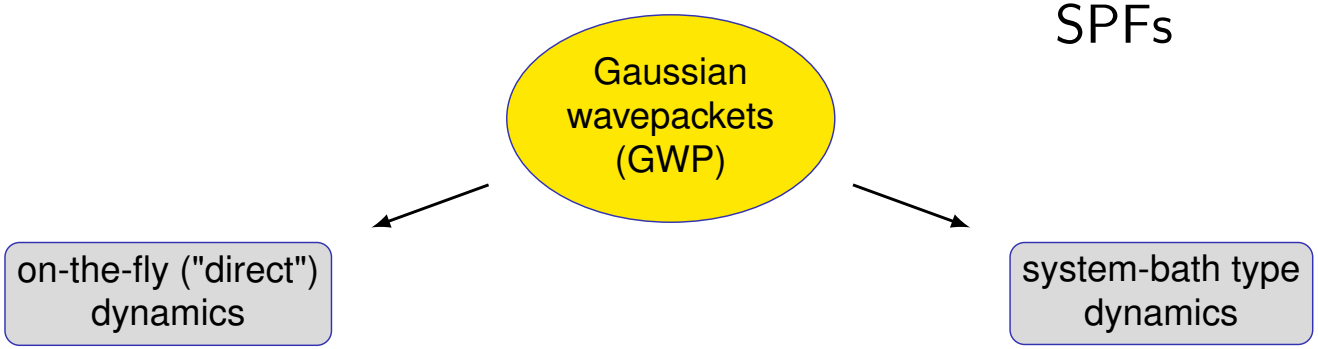

$\Psi(r,t) = \sum_j A_j(t) g_j(r,t)$ (vMCG)

Burghardt et al., JCP 119, 5364 (2003), 129, 174104 (2008)

variational Multi-Configurational Gaussians

Worth, Burghardt, Chem. Phys. Lett. 368, 502 (2003), Richings et al., Int. Rev. Phys. Chem., 34, 265 (2015)

- key precursors: Heller's Frozen and Thawed GWPs (1975, 1981 etc.)
- variational GWPs: Metiu & co (1985), Martinazzo & co (2007): LCSA (Local Coherent State Approximation)
- non-variational GWPs: Martínez & co (1996): FMS (Full Multiple Spawning); Shalashilin & co (2000): CCS (Coupled Coherent States); Batista & co (2003): MP/SOFT (Matching Pursuit)

G-MCTDH = Quantum-Semiclassical MCTDH

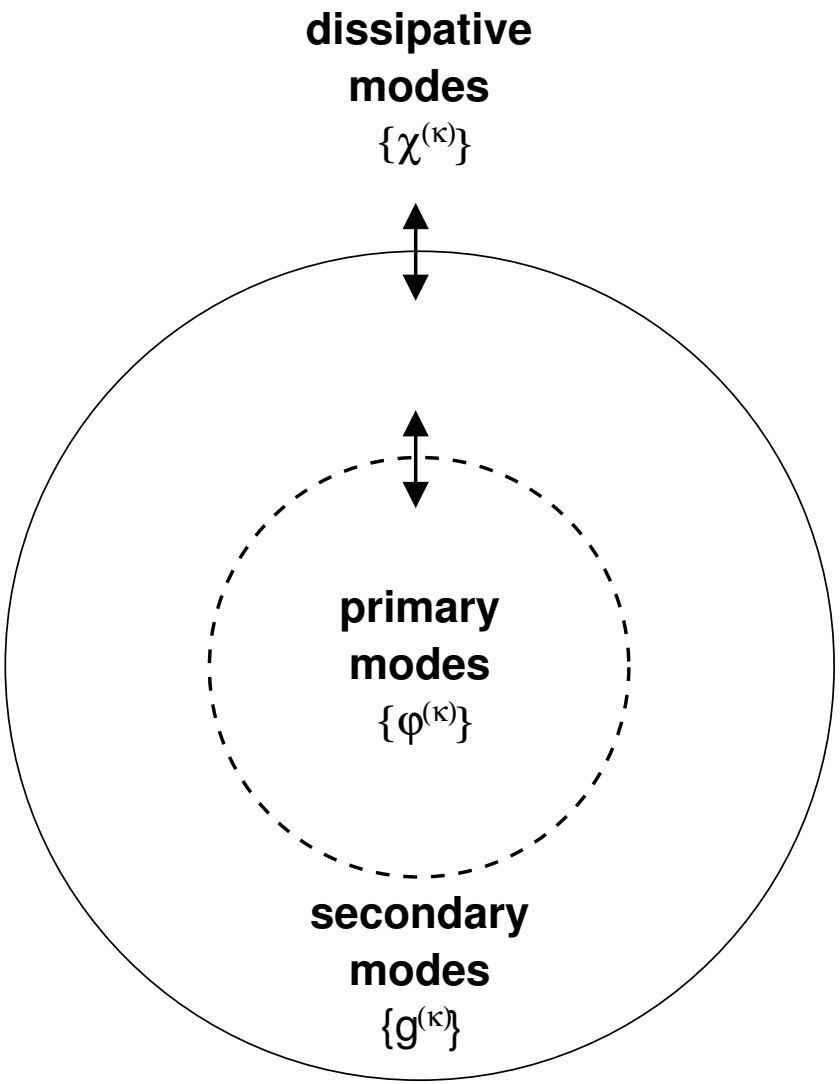

$$\Psi(r,t) = \sum_J A_J(t)\ \Phi_J(r,t)$$

$$\text{with } \Phi_J(r,t) = \prod_{\kappa=1}^{M} \varphi_{j_\kappa}^{(\kappa)}(r_\kappa,t)$$

Multi-Configuration Time-Dependent Hartree

Meyer et al., CPL **165**, 73 (1990), Beck et al., Phys. Rep. **324**, 1 (2000)

Gaussian-based hybrid method: G-MCTDH

$$\Phi_J(r,t) = \underbrace{\prod_{\kappa=1}^{M} \varphi_{j_\kappa}^{(\kappa)}(r_\kappa,t)}_{\text{primary nodes}} \quad \underbrace{\prod_{\kappa=M+1}^{P} g_{j_\kappa}^{(\kappa)}(r_\kappa,t)}_{\text{secondary modes}}$$

Burghardt, Meyer, Cederbaum, J. Chem. Phys. **111**, 2927 (1999)
Burghardt, Giri, Worth J. Chem. Phys. **129**, 174104 (2008)

Variational Dynamics

$$\Psi(r_1,\ldots,r_P,t) = \sum_{j_1}\cdots\sum_{j_P} A_{j_1\ldots j_P}(t) \prod_{\kappa=1}^{M} \varphi_{j_\kappa}^{(\kappa)}(r_\kappa,t) \prod_{\kappa=M+1}^{P} g_{j_\kappa}^{(\kappa)}(r_\kappa,t)$$

$$g_j^{(\kappa)}(r_\kappa,t) = \exp\left[r_\kappa \cdot a_j^{(\kappa)}(t) r_\kappa + \xi_j^{(\kappa)}(t)\cdot r_\kappa + \eta_j^{(\kappa)}(t)\right]$$

multidimensional Gaussian functions:

- "thawed" (TG) vs. "frozen" (FG)
- quasi-classical motion for $\xi_j = -2a_j q_j + i p_j$
- analytical integrals

Dirac-Frenkel variational principle:

$$\langle \delta\Psi | H - i\frac{\partial}{\partial t} | \Psi \rangle = 0 \longrightarrow \text{dynamical equations for } \Lambda_j^{(\kappa)} = (a_j^{(\kappa)}, \xi_j^{(\kappa)}, \eta_j^{(\kappa)})$$

- up to 50-100 modes – exponential scaling problem ($\sim f N^{f+1}$) is alleviated

Dynamical Equations

Burghardt, Meyer, Cederbaum, JCP 111, 2927 (1999)

coefficients: $$iS\dot{A} = \left[H - i\tau\right]A$$

SPFs (primary modes): $$i\dot{\varphi}^{(\kappa)} = \left(\hat{1} - \hat{P}^{(\kappa)}\right)\left[\rho^{(\kappa)}\right]^{-1}\hat{H}^{(\kappa)}\varphi^{(\kappa)}$$

GWPs (secondary modes): $$iC^{(\kappa)}\dot{\Lambda}^{(\kappa)} = Y^{(\kappa)}$$

$$S_{jl}^{(\kappa)} = \langle g_j^{(\kappa)} | g_l^{(\kappa)} \rangle \quad ; \quad \tau_{jl}^{(\kappa)} = \langle g_j^{(\kappa)} | \frac{\partial g_l^{(\kappa)}}{\partial t} \rangle$$

$$C_{j\alpha,l\beta}^{(\kappa)} = \rho_{jl}^{(\kappa)} \langle \frac{\partial g_j^{(\kappa)}}{\partial \lambda_{j\alpha}^{(\kappa)}} \Big| (\hat{1} - \hat{P}^{(\kappa)}) \Big| \frac{\partial g_l^{(\kappa)}}{\partial \lambda_{l\beta}^{(\kappa)}} \rangle \quad ; \quad Y_{j\alpha}^{(\kappa)} = \sum_l \langle \frac{\partial g_j^{(\kappa)}}{\partial \lambda_{j\alpha}^{(\kappa)}} \Big| (\hat{1} - \hat{P}^{(\kappa)}) \hat{H}_{jl}^{(\kappa)} \Big| g_l^{(\kappa)} \rangle$$

- evolution under multiconfigurational mean-field Hamiltonian
- coupled, variational equations for Gaussian parameters
- correlations between primary vs. secondary subspace
- analogous equations for density matrix evolution Burghardt, Meyer, Cederbaum, JCP 111, 2927 (1999)

Symplectic Structure of "VP Mechanics"

- variational formulation via action integral: $\delta \mathscr{S} = \delta \int dt \, \mathscr{L} = 0$

classical mechanics

$$\mathscr{L} = \sum_k p_k \dot{q}_k - H(q_k, p_k)$$

$$\dot{q}_k = \frac{\partial H}{\partial p_k}$$

$$\dot{p}_k = -\frac{\partial H}{\partial q_k}$$

VP mechanics

$$\mathscr{L} = \sum_{\alpha=1} \boldsymbol{S}^{(0\alpha)} \dot{\lambda}_\alpha - \langle \Psi | H | \Psi \rangle$$

identify: $\tilde{p}_\alpha = S^{(0\alpha)} = i \langle \Psi | \frac{\partial \Psi}{\partial \lambda_\alpha} \rangle$

$$\dot{\lambda}_\alpha = \frac{\partial \langle H \rangle}{\partial \tilde{p}_\alpha}$$

$$= \sum_\beta \frac{\partial \langle H \rangle}{\partial \lambda_\beta} \frac{\partial \lambda_\beta}{\partial \tilde{p}_\alpha}$$

$$= \sum_\beta \frac{\partial \langle H \rangle}{\partial \lambda_\beta} \left(C^{-1} \right)_{\alpha\beta}$$

Kramer, Saraceno, Geometry of the time-dependent variational principle, Springer (1981), Shalashilin, Burghardt, JCP 129, 084104 (2008)

Classical Evolution as a Special Case

$\boxed{q_j, p_j}$ $\longleftrightarrow$ $g_j(r_\kappa) = N_j \exp\left[(r_\kappa - q_j) \cdot a_j (r_\kappa - q_j) + i p_j \cdot (r_\kappa - q_j)\right]$

where we used $\xi_j = -2 a_j q_j + i p_j$

We have classical motion of $(q_j(t), p_j(t))$ if

- single Gaussian (cf. Heller)
- superposition of TGs / single-surface + harmonic potential: "decoupling effect" (Metiu & co, JCP (1985))

or

- if the classical limit is reached ($\lambda_{dB} \ll L$), such that G-MCTDH becomes a true mixed quantum-classical method for $\psi^\varepsilon = \sum_{jl} A_{jl} e^{iS_l/\varepsilon} \varphi_j g_l^\varepsilon$, see below

Römer, Burghardt, Mol. Phys. 111, 3618 (2013)

Implementation Details

- frozen Gaussians (FGs) almost exclusively used due to numerical robustness
- however, thawed Gaussians (TGs) were successfully employed for system-bath problems
  [Burghardt, Nest, Worth (2003)]
- various conventions possible for complex GWP phase η_j: here, normalized GWPs, imaginary part of phase set to zero
- local harmonic approximation (LHA) or higher-order local expansion

- split off separable part of evolution: $i\dot{\Lambda}^{(\kappa)} = X_0^{(\kappa)} + (C^{(\kappa)})^{-1} Y_{\mathrm{corr}}^{(\kappa)}$
- singularities of the $\boldsymbol{S}$ and $\boldsymbol{C}$ matrices (linear dependencies): standard regularization scheme
- Wigner sampling or single GWP as initial condition
- Coupled electronic states: no surface hopping, no spawning
- dynamic GWP allocation (G. Worth)
- direct-dynamics implementation: DD-vMCG/Quantics (G. Worth)

G-MCTDH Calculation for S_2/S_1 CoIn in pyrazine

Hybrid calculation for 4+20 modes (FGs)

absorption spectrum

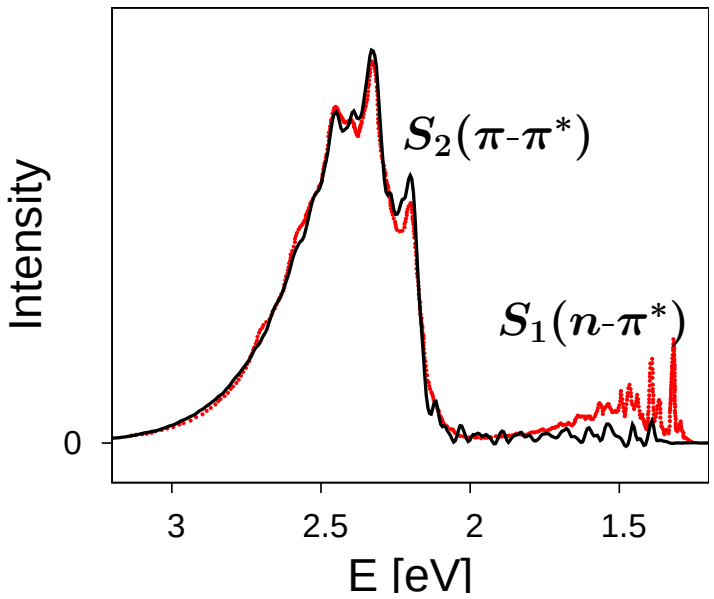

FT

autocorrelation function

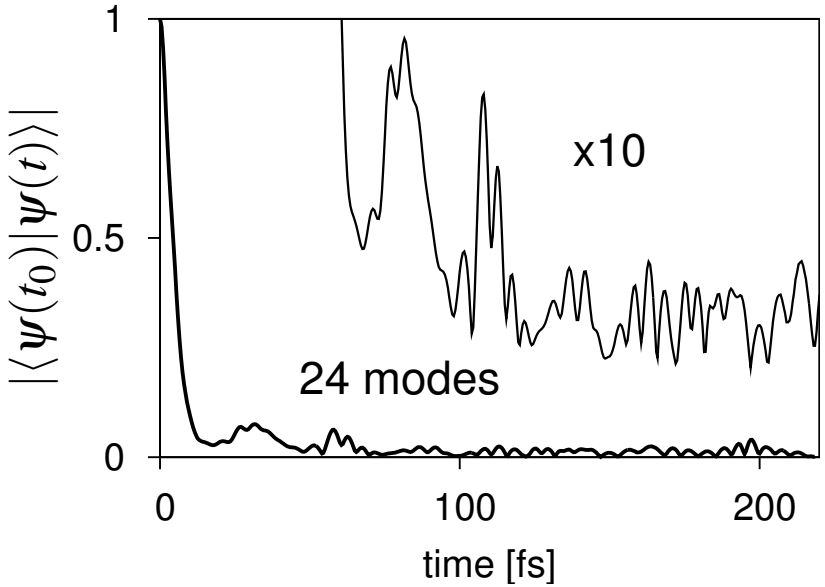

dotted red line: experiment

Yamazaki et al., Faraday Discuss. **75**, 395 (1983)

full black line: G-MCTDH

Burghardt, Giri, Worth, JCP **129**, 174104 (2008)

state 1: $([19,10]_{\text{core}}, [18,10,18,10]_{\text{bath}})$

state 2: $([12,7]_{\text{core}}, [10,8,12,10]_{\text{bath}})$

150 fs / 1644 MB / 1250 hrs / 6962400 config's

MCTDH: 150 fs / 2614 MB / 279 hrs / 10966760 cf's

vMCG Calculation for S_2/S_1 CoIn in pyrazine

GWP-only calculation[2] for 4 modes (FGs)

left: S_2 population, right: autocorrelation red: MCTDH reference

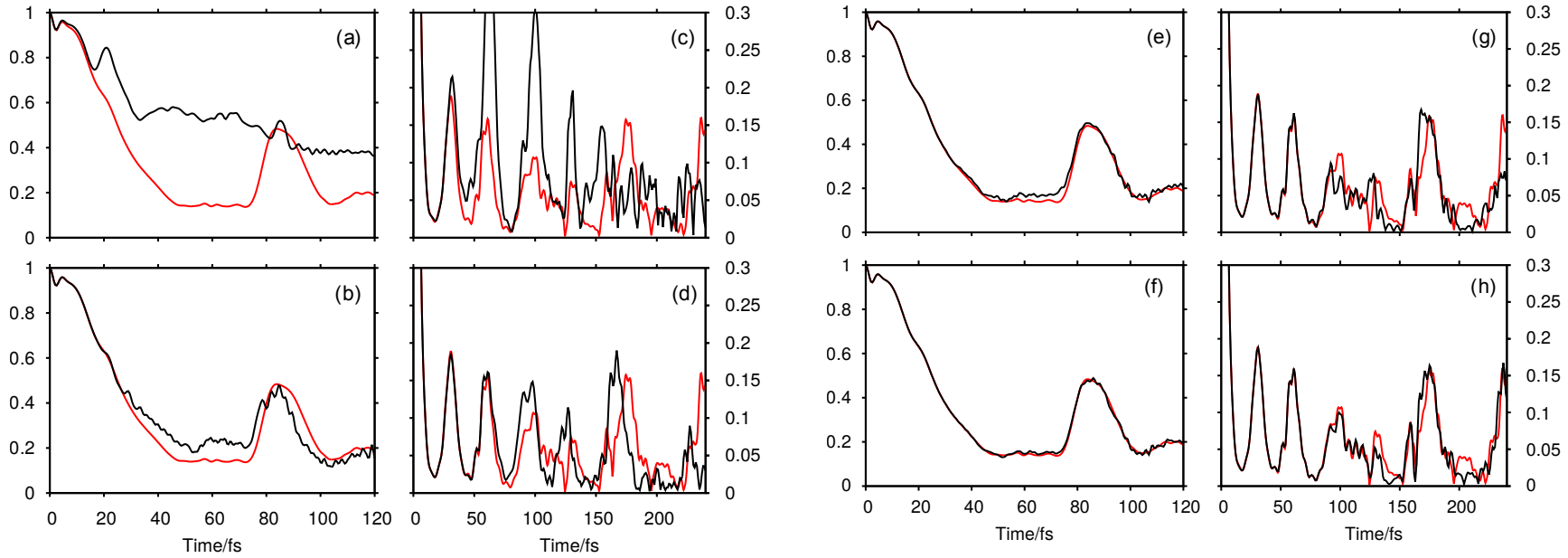

- (a), (c): 140 classical GWPs
- (b), (d): 20 vMCG GWPs
- (e), (g): 40 vMCG GWPs
- (f), (h): 60 vMCG GWPs

Richings et al., Int. Rev. Phys. Chem., 34, 265 (2015), Burghardt, Giri, Worth J. Chem. Phys. **129**, 174104 (2008)

[2] single-set calculations, i.e., shared GWP basis for both states (multi-set performs similarly)

Topics

Two-Layer G-MCTDH – Motivation

- original G-MCTDH concept: combined, correlated TG modes (correlations through off-diagonal elements of the width matrix)
- in practice: G-MCTDH or vMCG using combined FG modes
  - factorizable, uncorrelated FG configurations
  - despite the separability, the C matrix is *not* block-diagonal
  - hence, expensive inversion step $\propto (\tilde{n}d)^3$
- alternative concept: replace high-dimensional FG's by superpositions of FG configurations $\longrightarrow$ two-layer approach

Two-Layer (2L)-G-MCTDH Scheme

Römer, Ruckenbauer, Burghardt, J. Chem. Phys. 138, 064106 (2013)

$$\Psi(r,t) = \sum_J A_J(t)\Phi_J(r,t) \;\; = \sum_J A_J(t) \prod_{\kappa=1}^{M} \varphi_{j_\kappa}^{(\kappa)}(r_\kappa,t)$$

where the single-particle functions (SPFs) $\varphi_{j_\kappa}^{(\kappa)}$ are now built as superpositions of Frozen Gaussian (FG) configurations,

$$\begin{aligned} \varphi_{j_\kappa}^{(\kappa)}(r_\kappa,t) &= \sum_L B_{j,L}^{(\kappa)}(t) G_L^{(\kappa)}(r_\kappa,t) \\ &= \sum_L B_{j,L}^{(\kappa)}(t) \prod_\mu g_{l_\mu}^{(\kappa,\mu)}(r_{\kappa_\mu},t) \end{aligned}$$

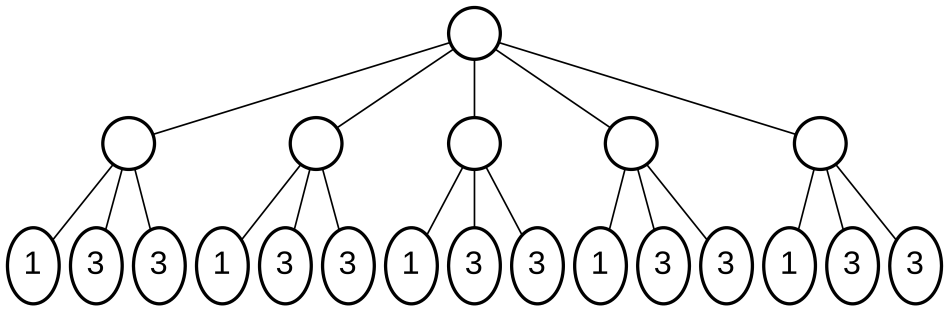

- hierarchical Tucker format
- intra-SPF correlations are carried by B coefficients
- GWP parameter dynamics in small (κ,μ) subspaces
- first-layer SPFs can be chosen to be orthogonal: $\langle \varphi_j^{(\kappa)}(t) | \varphi_{j'}^{(\kappa)}(t) \rangle = \delta_{jj'}$

Two-Layer G-MCTDH – Equations of Motion

1st layer coefficients: $$i\dot{A} = HA$$

2nd layer coefficients: $$iS^{(\kappa)}\dot{B}^{(\kappa)} = \left[\tilde{H}^{(\kappa)} - i\tilde{\tau}^{(\kappa)}\right] B^{(\kappa)}$$

GWPs (2nd layer): $$iC^{(\kappa,\mu)}\dot{\Lambda}^{(\kappa,\mu)} = Y^{(\kappa,\mu)}$$

where $\tilde{S}^{(\kappa)}_{jL,j'L'} = \delta_{jj'}\langle G^{(\kappa)}_L | G^{(\kappa)}_{L'}\rangle$, $\tilde{\tau}^{(\kappa)}_{jL,j'L'} = \delta_{jj'}\langle G^{(\kappa)}_L | \partial_t G^{(\kappa)}_{L'}\rangle$

and the 1st layer mean field term: $\tilde{H}^{(\kappa)}_{jL,j'L'} = \langle G^{(\kappa)}_L | (1-\hat{P}^{(\kappa)}) \left[(\rho^{(\kappa)})^{-1}\hat{H}^{(\kappa)}\right]_{jj'} G^{(\kappa)}_{L'}\rangle$

and for the parameter equations: $C^{(\kappa,\mu)}_{j\alpha,l\beta} = \rho^{(\kappa,\mu)}_{jl}\langle \partial_\alpha g^{(\kappa,\mu)}_j | (\hat{1}-\hat{P}^{(\kappa,\mu)}) | \partial_\beta g^{(\kappa,\mu)}_l\rangle$

as well as $Y^{(\kappa,\mu)}_{j\alpha} = \sum_l \langle \partial_\alpha g^{(\kappa,\mu)}_j | (\hat{1}-\hat{P}^{(\kappa,\mu)})\hat{H}^{(\kappa,\mu)}_{jl} | g^{(\kappa,\mu)}_l\rangle$

Römer, Ruckenbauer, Burghardt, J. Chem. Phys. 138, 064106 (2013)

Two-Layer G-MCTDH – Scaling

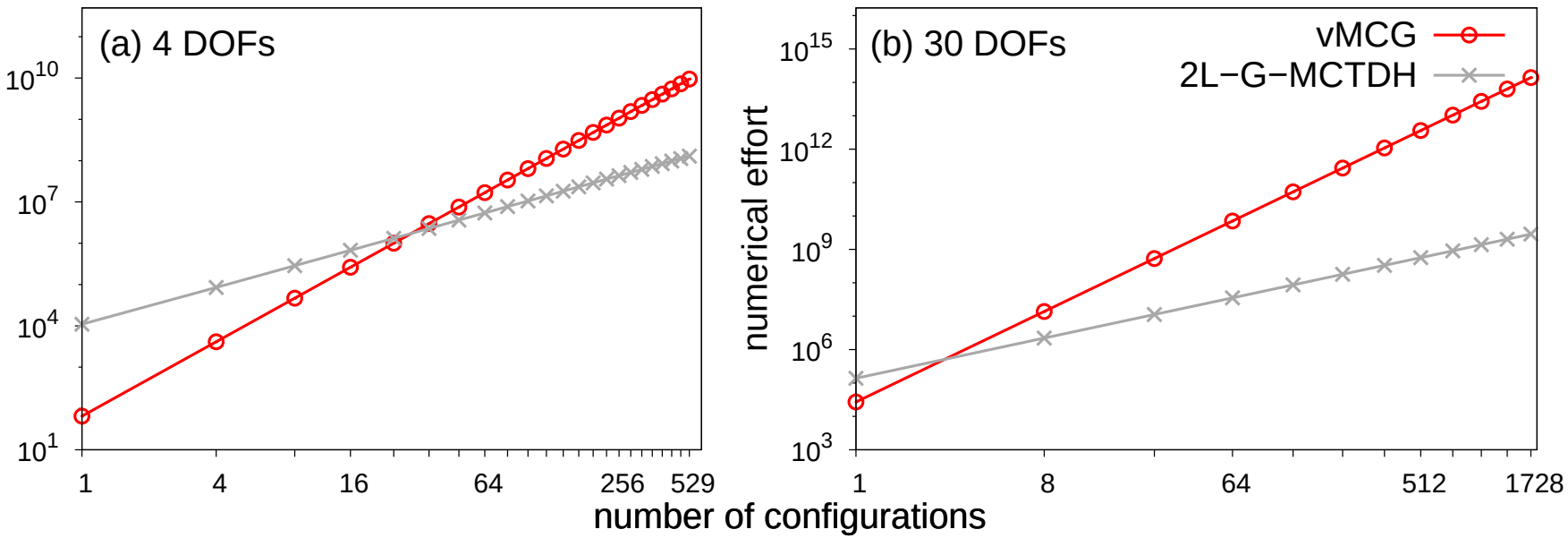

effort$^{\text{G-MCTDH}} \sim mf^2n^{f+1} + f(\tilde{d}n)^3$

calculation of mean fields + C matrix inversion

effort$^{\text{2L-G-MCTDH}} \sim m_1f_1^2n_1^{f_1+1} + m_1m_2f_1f_2n_1n_2^{f_2+1}(f_2+n_1) + f_1f_2(d_2n_2)^3$

calculation of 1st and 2nd-layer mean fields + C matrix inversion

2L-G-MCTDH for Coupled Electronic States: Three Variants

— single-set: shared basis

$$\Psi_S(r,t) = \sum_{J,s} A_{Js}(t)\Phi_J(r,t)|s\rangle = \sum_{J,s} A_{Js}(t)\prod_{\kappa=1}^{N}\varphi_{j_\kappa}^{(\kappa)}(r_\kappa,t)|s\rangle$$

$$\varphi_{j_\kappa}^{(\kappa)}(r_\kappa,t) = \sum_L B_{j,L}^{(\kappa)}(t)G_L^{(\kappa)}(r_\kappa,t) = \sum_L B_{j,L}^{(\kappa)}(t)\prod_\mu g_{l_\mu}^{(\kappa,\mu)}(r_{\kappa_\mu},t)$$

— multi-set: state-specific basis

$$\Psi_M(r,t) = \sum_{J,s} A_J^{(s)}(t)\Phi_J^{(s)}(r,t)|s\rangle = \sum_{J,s} A_J^{(s)}(t)\prod_{\kappa=1}^{N}\varphi_{j_\kappa}^{(\kappa,s)}(r_\kappa,t)|s\rangle$$

$$\varphi_{j_\kappa}^{(\kappa,s)}(r_\kappa,t) = \sum_L B_{j,L}^{(\kappa,s)}(t)G_L^{(\kappa,s)}(r_\kappa,t) = \sum_L B_{j,L}^{(\kappa,s)}(t)\prod_\mu g_{l_\mu}^{(\kappa,\mu,s)}(r_{\kappa_\mu},t)$$

— hybrid-multi/single set ≡ hybrid-set: state-specific but shared 2nd-layer basis

$$\Psi_H(r,t) = \sum_{J,s} A_J^{(s)}(t)\Phi_J^{(s)}(r,t)|s\rangle = \sum_{J,s} A_J^{(s)}(t)\prod_{\kappa=1}^{N}\varphi_{j_\kappa}^{(\kappa,s)}(r_\kappa,t)|s\rangle$$

$$\varphi_{j_\kappa}^{(\kappa,s)}(r_\kappa,t) = \sum_L B_{j,L}^{(\kappa,s)}(t)G_L^{(\kappa)}(r_\kappa,t) = \sum_L B_{j,L}^{(\kappa,s)}(t)\prod_\mu g_{l_\mu}^{(\kappa,\mu)}(r_{\kappa_\mu},t)$$

Coupled Electronic States: Single-Set, Multi-Set, Hybrid-Set

Example: 20-mode calculation for donor-acceptor system

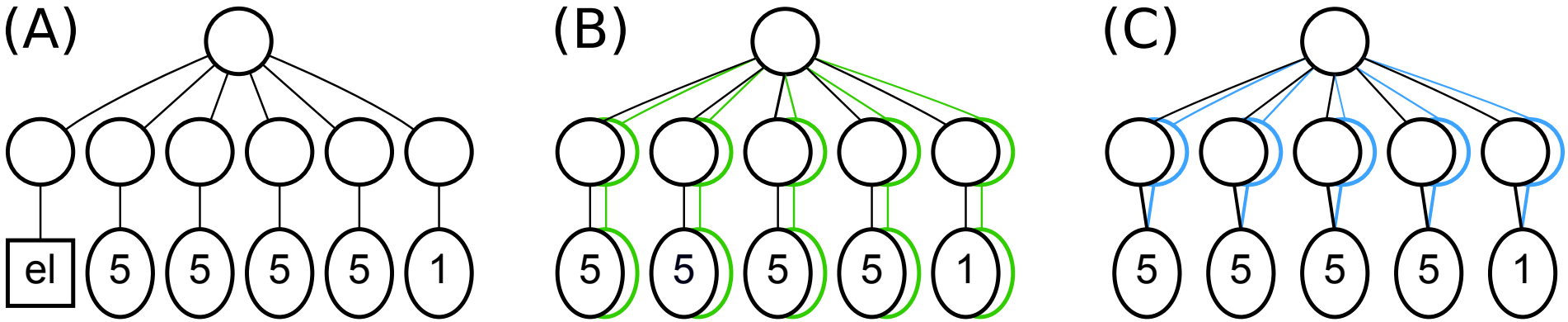

Eisenbrandt, Ruckenbauer, Burghardt, submitted (2018)

- (A) single-set (B) multi-set (C) hybrid single/multi-set
- convergence properties can differ significantly depending on the system

Benchmarks for 2-State Donor-Acceptor Model

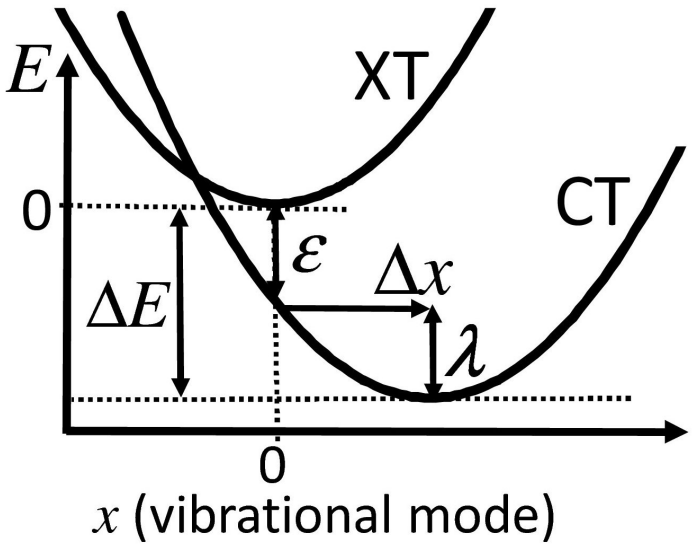

$$\hat{H} = \hat{H}_0 + \hat{H}_R + \hat{H}_B$$

$\hat{H}_0$: electronic part
$\hat{H}_R$: inter-fragment coordinate part
$\hat{H}_B$: phonon bath part

$$\hat{H}_0 = \Delta_{\mathrm{XT-CT}} |\mathrm{CT}\rangle\langle\mathrm{CT}| + \gamma\left(|\mathrm{XT}\rangle\langle\mathrm{CT}| + |\mathrm{CT}\rangle\langle\mathrm{XT}|\right)$$

$$\hat{H}_R = \frac{\omega_R}{2}(\hat{R}^2 + \hat{P}^2) + \kappa_R \hat{R}\,|\mathrm{CT}\rangle\langle\mathrm{CT}| + \gamma_R \hat{R}\left(|\mathrm{XT}\rangle\langle\mathrm{CT}| + |\mathrm{CT}\rangle\langle\mathrm{XT}|\right)$$

$$\hat{H}_B = \sum_{i=1}^{N} \frac{\omega_i}{2}(\hat{x}_i^2 + \hat{p}_i^2) + \sum_{i=1}^{N} \kappa_i x_i\,|\mathrm{CT}\rangle\langle\mathrm{CT}| + \sum_{i=1}^{N} \frac{\kappa_i^2}{2\omega_i}$$

Tamura, Martinazzo, Ruckenbauer, Burghardt, J. Chem. Phys., 137, 22A540 (2012)

Spectral Densities from Electronic Structure Calculations(*)

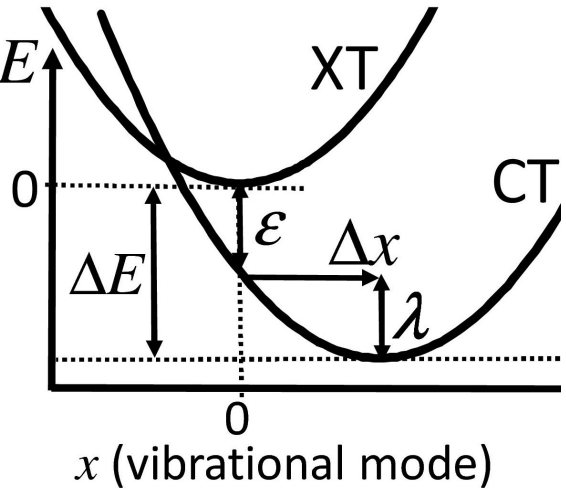

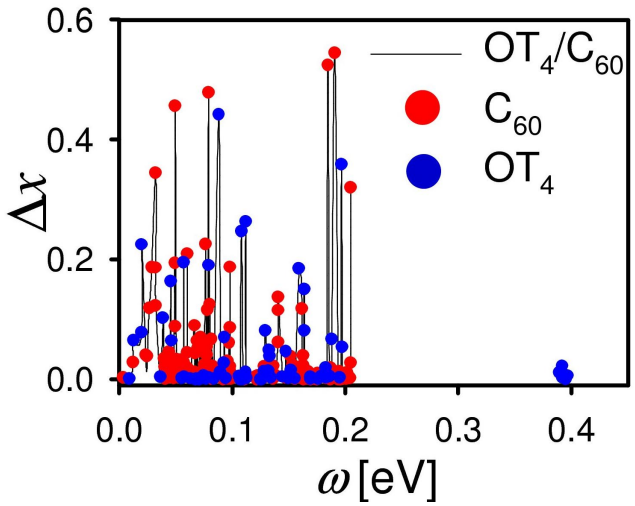

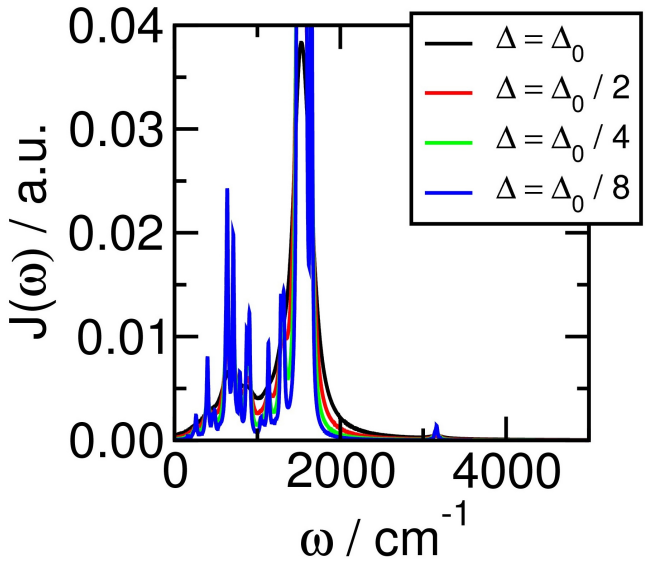

$$J(\omega) = \frac{\pi}{2} \sum_n^N \frac{c_n^2}{\omega_n} \delta(\omega - \omega_n) \simeq \frac{\pi}{2} \sum_n^N \frac{c_n^2}{\pi} \frac{\Delta}{(\omega - \omega_n)^2 + \Delta^2}$$

Tamura, Martinazzo, Ruckenbauer, Burghardt, J. Chem. Phys., 137, 22A540 (2012)

(*)NB. Alternatively: obtain SD's from correlation functions (MD, CPMD, . . .)

P3HT/PCBM Model Including CTX States

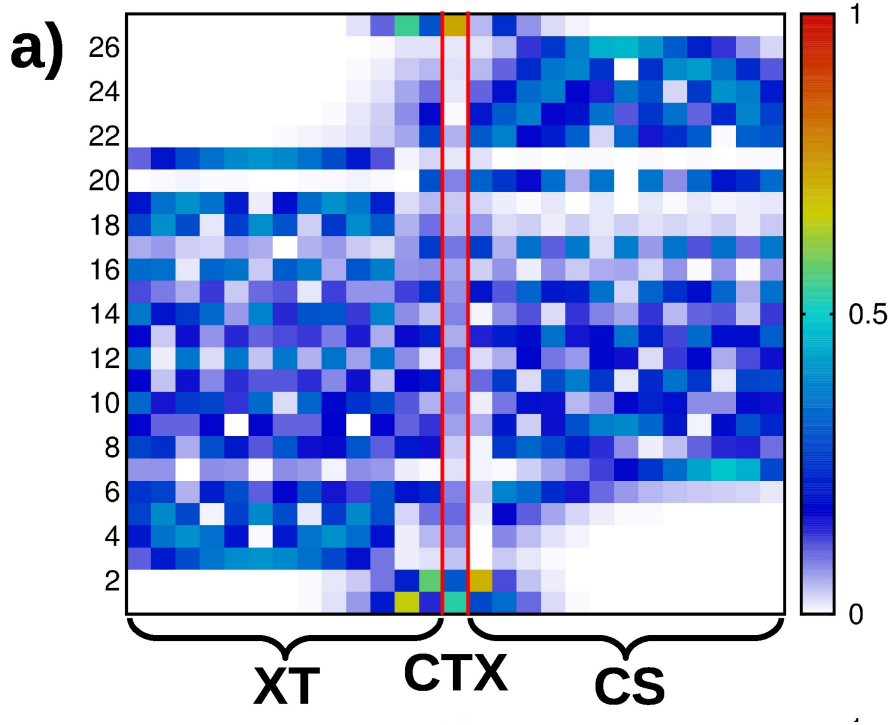

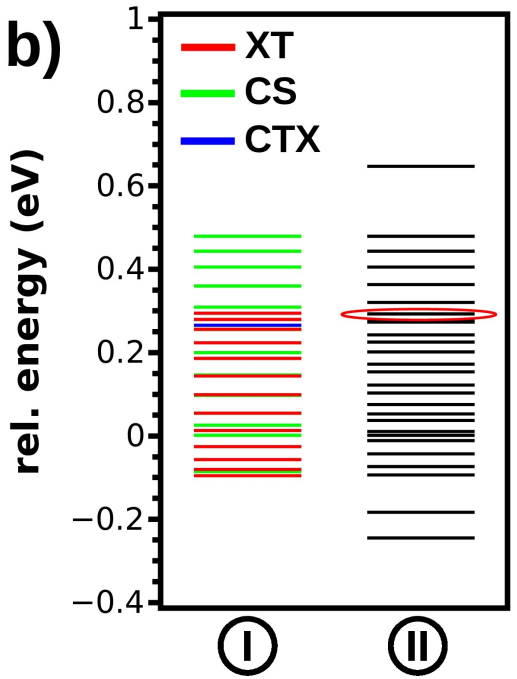

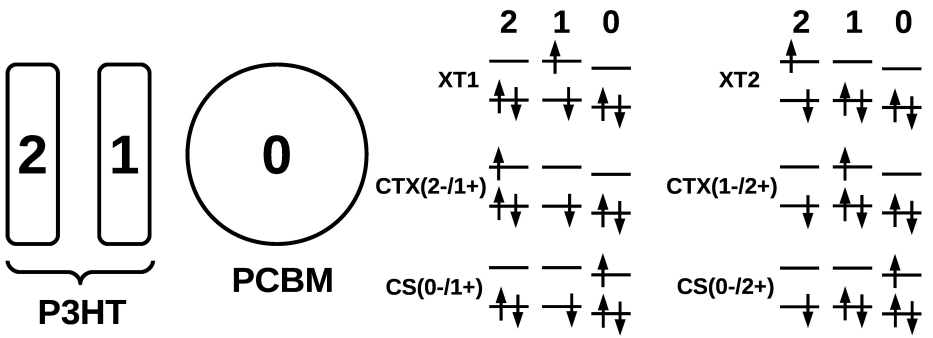

- 182 states/112 modes
- OT charge transfer excitons open new pathways for carrier formation
- but also act as energetic traps

Polkehn, Tamura, Burghardt, J. Phys. B, 51, 014003 (2018)

Ultrafast Coherent Transfer Dynamics (MCTDH/60 Modes)

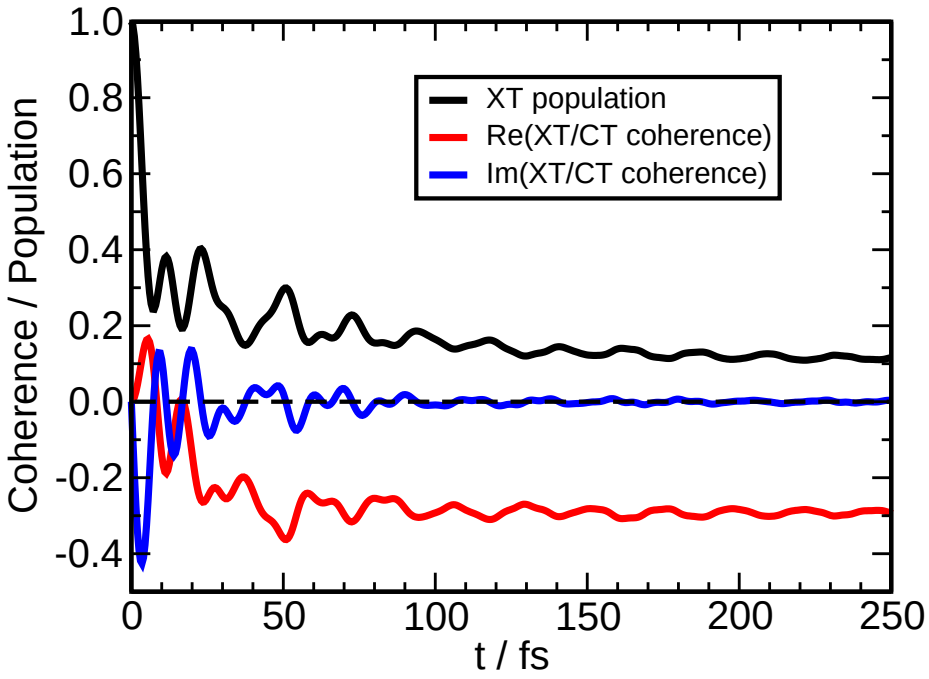

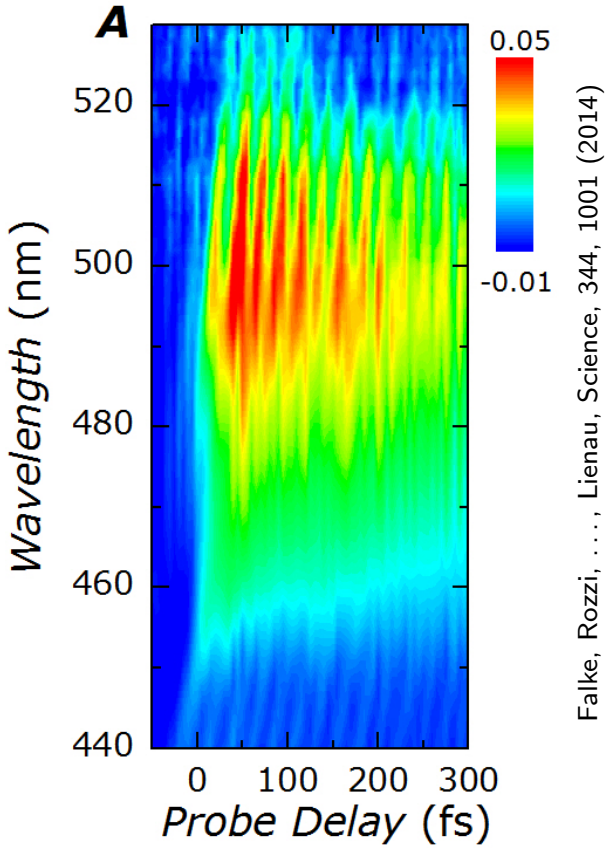

el. coherence: $\rho_{XT,CT}(t) = \mathrm{Tr}\{|\mathrm{CT}\rangle\langle\mathrm{XT}|\hat{\rho}(t)\}$

- imaginary part $(-2\gamma/\hbar)\mathrm{Im}\rho_{XT,CT}$ ⟷ population flux
- real part ⟷ stationary coherent superposition ($P_{\mathrm{XT}} \sim 0.1$, $P_{\mathrm{CT}} \sim 0.9$)
- experiment: ultrafast ET (~ 50 fs), oscillatory features [Brabec et al., CPL (2001)]) confirmed by recent pump-probe experiments by Lienau group [Science (2014)])

Benchmarks – 41D Donor-Acceptor System

vMCG (FGs)

- 2 el. states, 1 subsystem mode, 40 bath modes
- qualitative agreement even of "cheap" calculations
- memory requirements favorable
- vMCG very expensive even for few config's

	calc. type	mode combination	# configs	memory [mb]	CPU time [hh:mm]	C inversion avg/tot time
1	MCTDH	[6,8],[6,8],[3,5],[2,3] [2,2],[2,2],[2,2],[2,2],[6,8]	143616	754	1:36	- -
2	vMCG 2,2	[2,2]	4	2	0:47	5.10 ms 0:03:60
3	vMCG 6,6	[6,6]	12	15	7:10	136.38 ms 1:29:18
4	vMCG 12,12	[12,12]	24	55	47:56	1758.71 ms 23:21:38

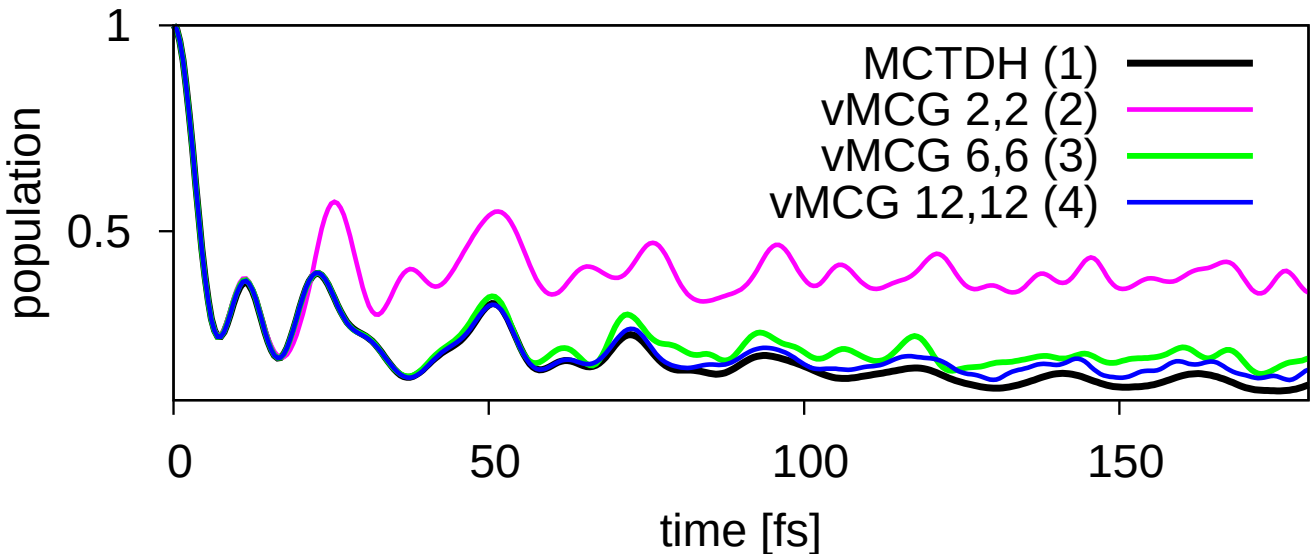

Benchmarks – 41D Donor-Acceptor System

G-MCTDH (FGs)

- different mode combinations and #'s of GWP config's
- C inversion in smaller subspaces
- all G-MCTDH calculations have reasonable timings
- memory requirements favorable

	calc. type	mode combination	# configs	memory [mb]	CPU time [hh:mm]	C inversion avg/tot time
1	MCTDH	[6,8],[6,8],[3,5],[2,3] [2,2],[2,2],[2,2],[2,2],[6,8]	143616	754	1:36	- -
2	G-MCTDH hybrid	[6,8],[6,8],[3,5],[2,3] [2,2],[2,2],[2,2],[2,2],[6,8]	143616	28	0:12	0.21 ms 0:01:48
3	G-MCTDH hybrid	[8,10],[8,10],[5,7],[4,5] [3,3],[3,3],[3,3],[3,3],[6,8]	2890080	521	3:56	7.65 ms 0:12:03
4	G-MCTDH all-GWP	[6,8],[6,8],[3,5],[2,3] [2,2],[2,2],[2,2],[2,2],[6,8]	143616	28	0:26	0.19 ms 0:06:13

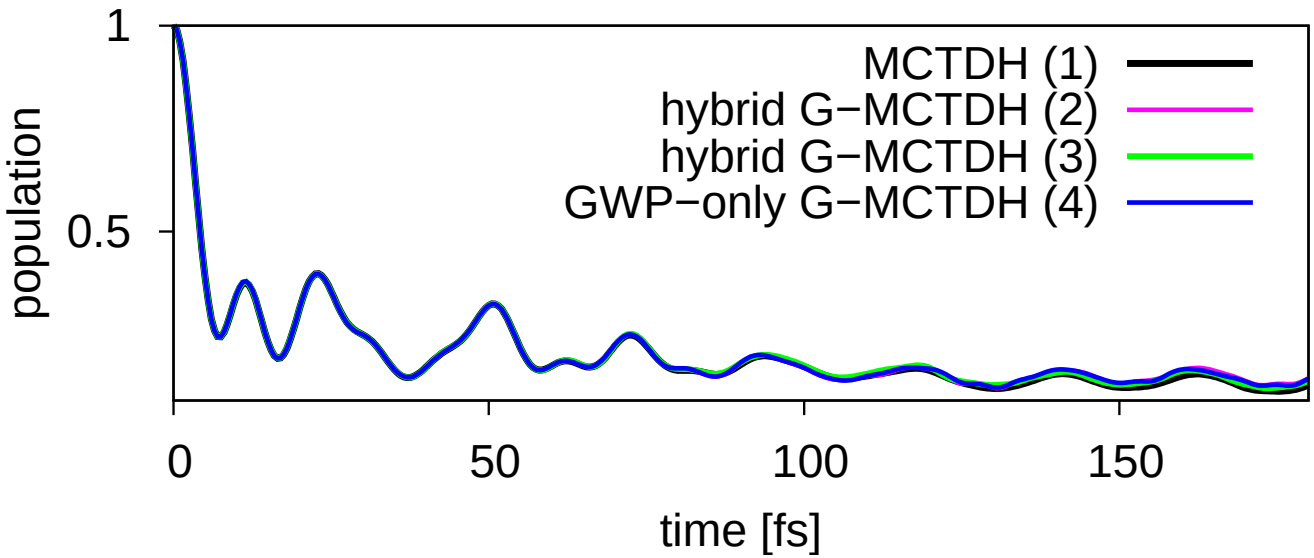

Benchmarks – 100D Donor-Acceptor System

2L-GMCTDH (FGs)

single-set calc's;
rediscretized SDs for
20 / 100 modes

Eisenbrandt, Ruckenbauer,
Burghardt, submitted (2018)

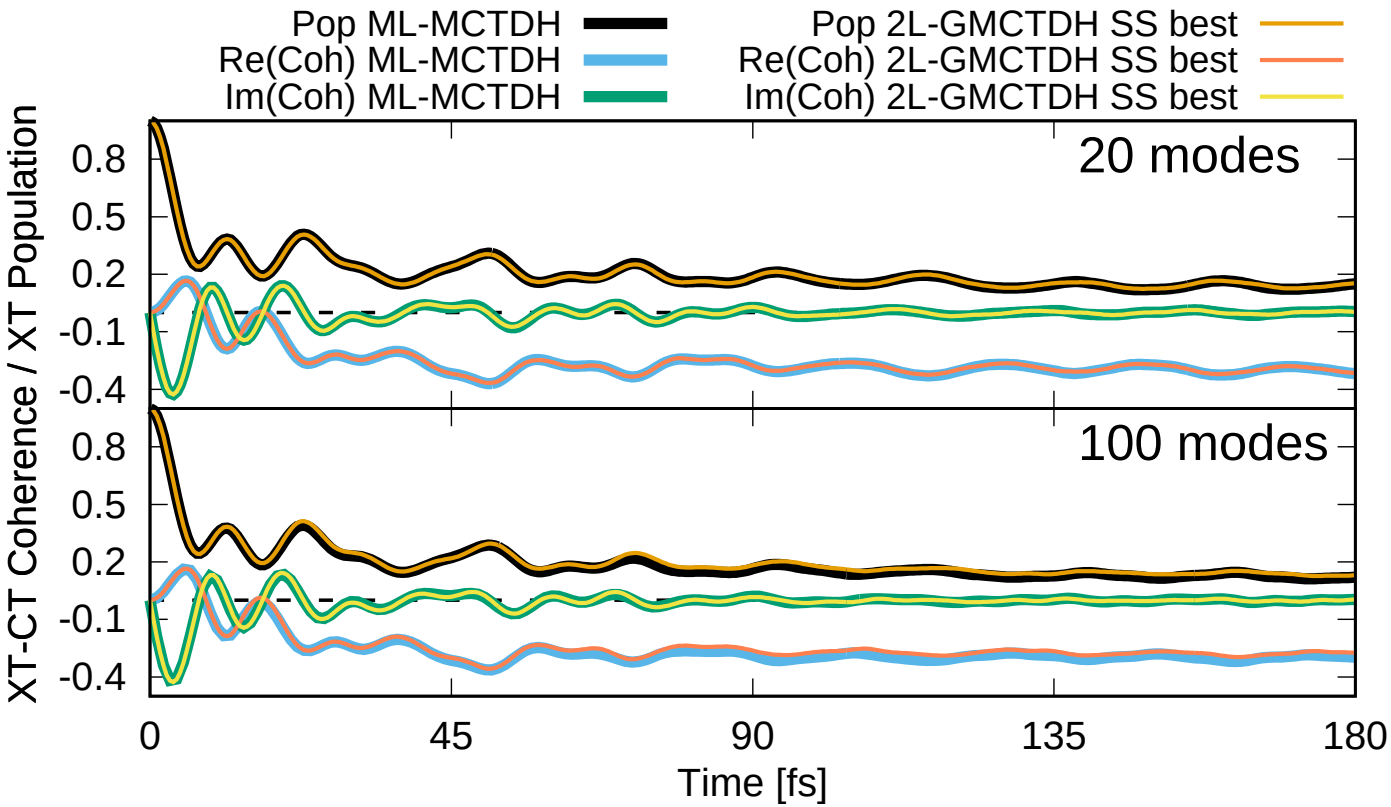

20 modes / single-set 2L-GMCTDH (180 fs): CPU = 6527 s, 7513 steps, 0.86 s/step, 40 MB RAM

20 modes / single-set 2L-MCTDH (180 fs): CPU = 33653 s, 8199 steps, 4.1 s/step, 308 MB RAM

100 modes / single-set 2L-GMCTDH (200 fs): CPU = 16209 s, 30348 steps, 0.53 s/step, 94 MB RAM

100 modes / single-set 2L-MCTDH (200 fs): CPU = 303130 s, 10655 steps, 28.45 s/step, 2462 MB RAM

100 modes / single-set 6L-MCTDH (200fs): CPU = 40380 s, 17710 steps, 2.28 s/step, 15 MB RAM

2L-GMCTDH: Two-Layer Trees (Single-Set)

20 modes

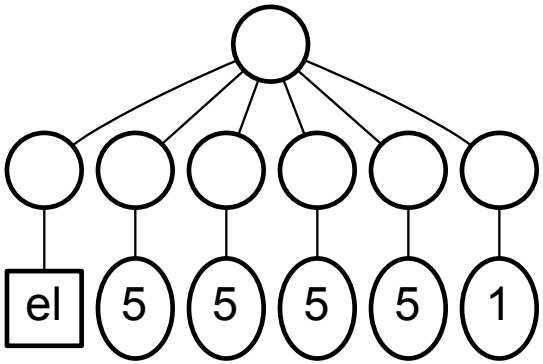

100 modes

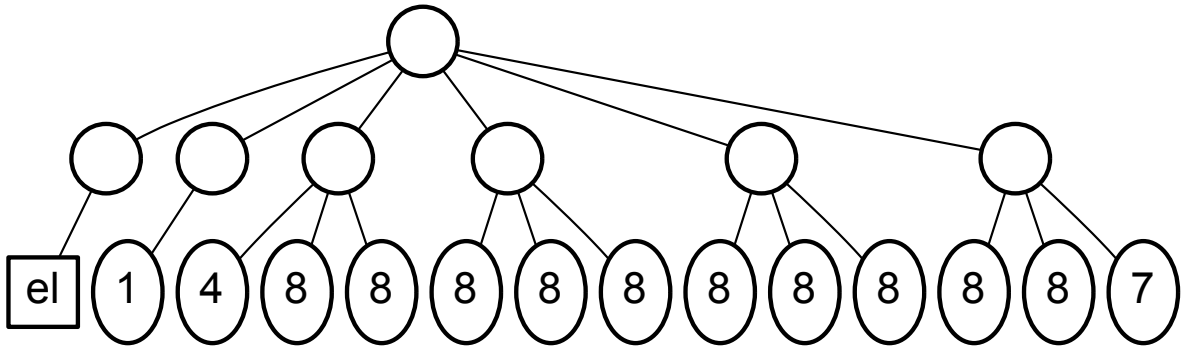

Eisenbrandt, Ruckenbauer, Burghardt, submitted (2018)

- 20 modes: 1st-layer and 2nd-layer modes have the same number of DOFs
  1st-layer SPFs: [8], [8], [8], [8], [10]
  2nd-layer SPFs: [8], [8], [8], [8], [10]
- 100 modes: 1st-layer modes split up into 2nd-layer modes with up to 8 DOFs
  1st-layer SPFs: [7], [5], [5], [5], [7]
  2nd-layer SPFs: [8], [5,5,5], [4,4,3], [4,4,4], [4,4,4]

2L-GMCTDH: Comparison Single-/Multi-/Hybrid-Set

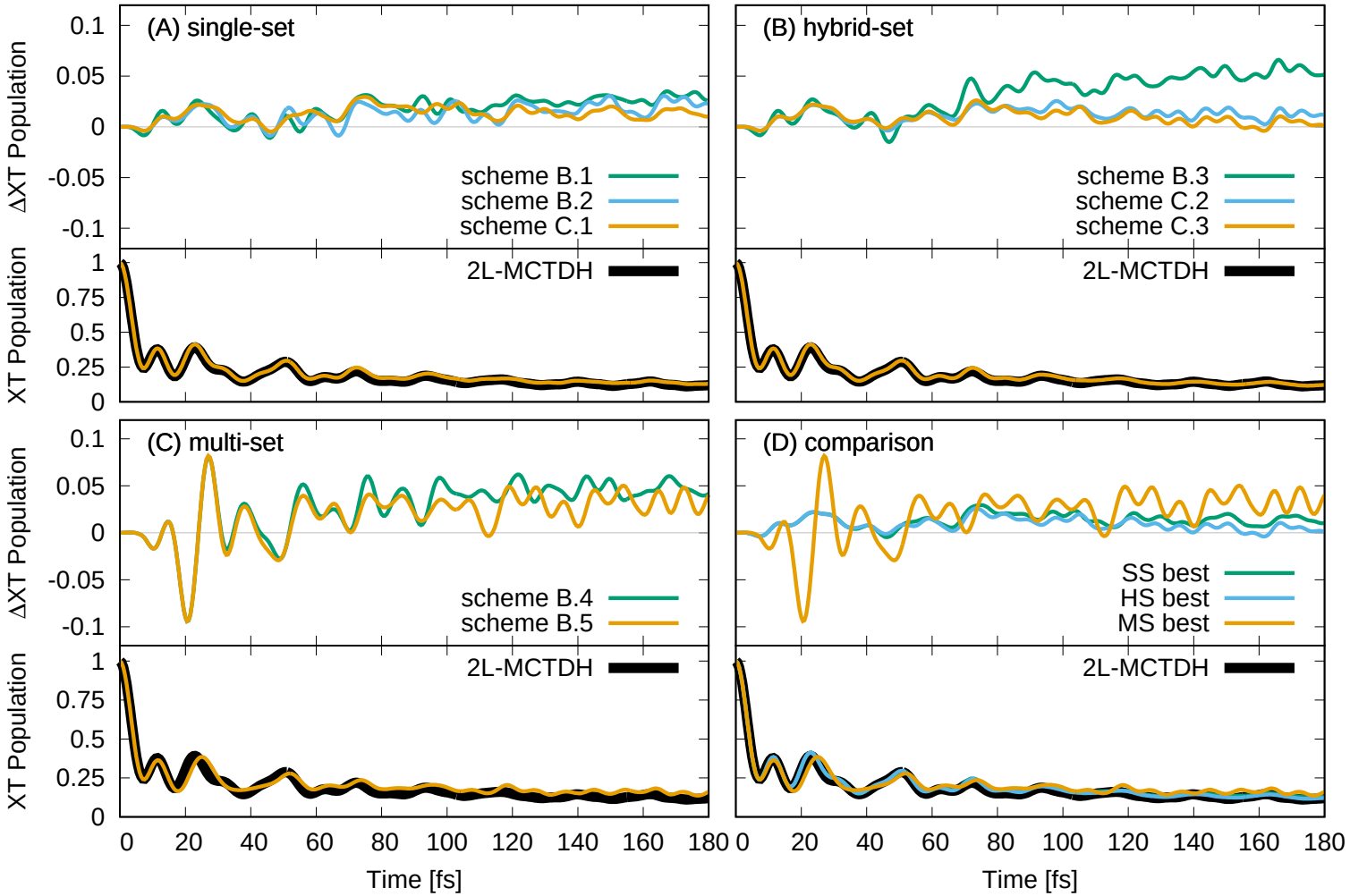

- for 100 modes, single-set exhibits best convergence, followed by hybrid-set

Implementation & Scaling

- in-house code (M. Ruckenbauer, P. Eisenbrandt)
- general polynomial potentials
- Hamiltonian given as sum-over-products
- initial condition: shell-like spatial distribution (here, initially unoccupied GWPs narrower than central GWP)
- conventional regularization of $\boldsymbol{S}$ and $\boldsymbol{C}$ matrices
- ABM integrator (time step typically $\sim 10^{-2}$ fs)
- scaling in good agreement with theory

- NB: joint standard G-MCTDH/vMCG code with G. A. Worth now available within QUANTICS package at `http://ccpforge.cse.rl.ac.uk/`.

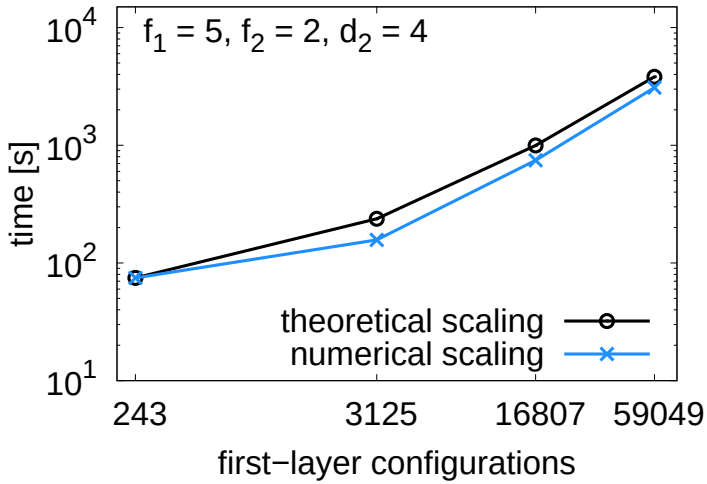

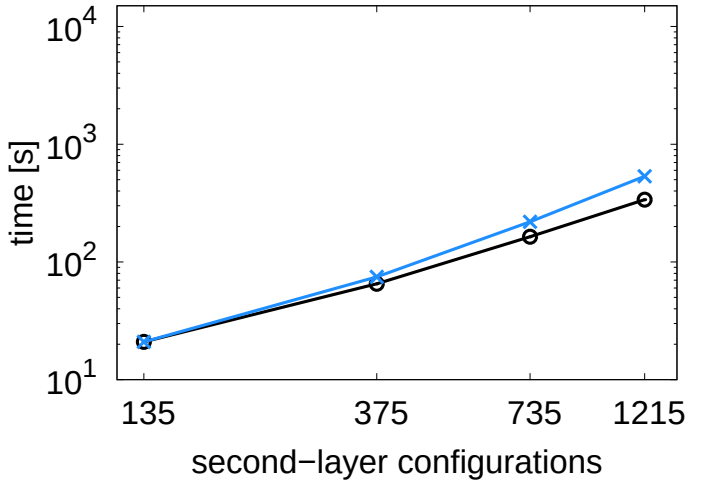

Multi-Layer Form

$$\Psi(t) = \sum_J A_J^{[1]}(t)\Phi_J^{[1]}(t) := \sum_J A_J^{[1]}(t) \prod_{\kappa_1=1}^{f^{[1]}} \chi_{j_{\kappa_1}}^{[1](\kappa_1)}(t)$$

with the spf's of the first $M-1$ layers ($m \in \{2,3,\ldots,M\}$),

$$\chi_j^{[m-1](\mu_m-1)}(t) \quad = \quad \sum_J A_{j,J}^{[m](\mu_m-1)}(t)\Phi_J^{[m](\mu_m-1)}(t) = \sum_J A_{j,J}^{[m](\mu_m-1)}(t) \prod_{\kappa_m=1}^{f_{\mu_{m-1}}^{[m]}} \chi_{j_{\kappa_m}}^{[m]}(t)$$

and the final (Mth) layer composed of FG's,

$$\chi_j^{[M](\mu_M)}(t) = g_j^{(\mu_M)}(\Lambda_j^{(\mu_M)}(t))$$

can be straightforwardly combined with existing ML-MCTDH approaches

Römer, Ruckenbauer, Burghardt, J. Chem. Phys. 138, 064106 (2013)

Topics

Quantum-Classical Limit of G-MCTDH

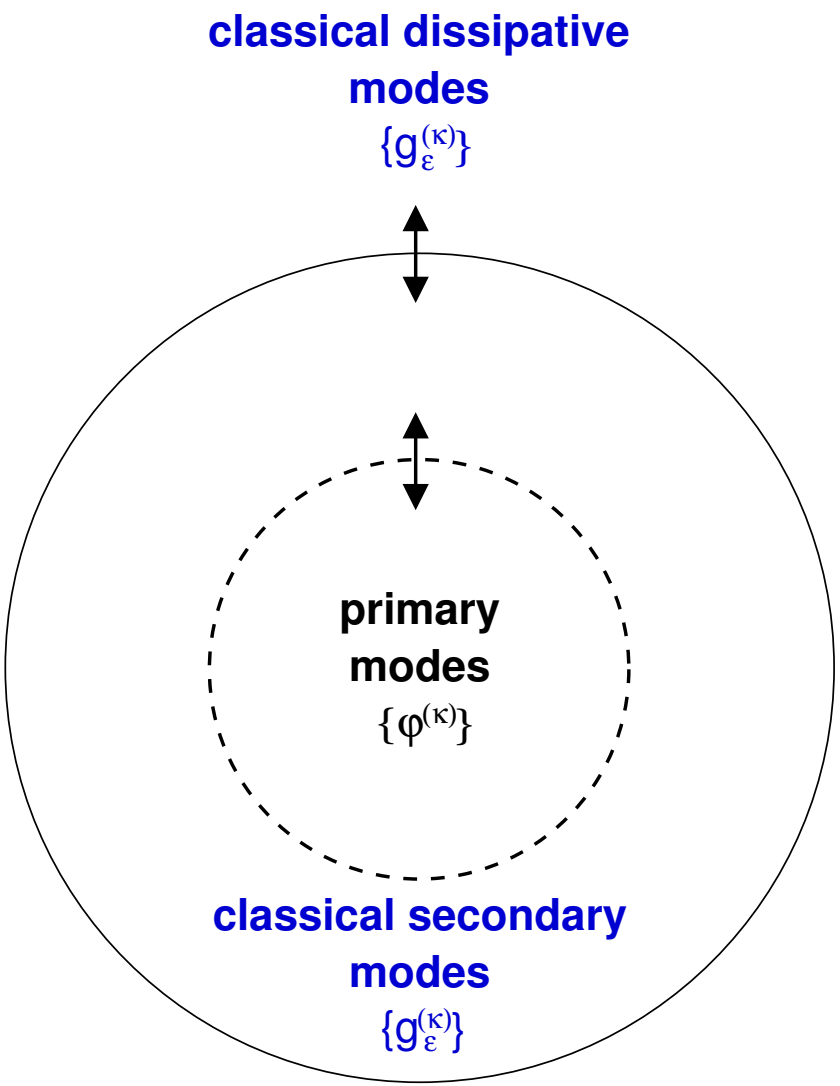

take GWP subspace to classical limit:

$$\Psi^{\mathrm{qc}}(r,t) = \sum_J A_J(t)\ \Phi_J^{\mathrm{qc}}(r,t)$$

$$\Phi_J^{\mathrm{qc}}(r,t) = \underbrace{\prod_{\kappa=1}^{M} \varphi_{j_\kappa}^{(\kappa)}(r_\kappa,t)}_{\text{primary nodes}}\ \underbrace{\prod_{\kappa=M+1}^{P} g_{\varepsilon,j_\kappa}^{(\kappa)}(r_\kappa,t)}_{\text{secondary modes}}$$

Römer, Burghardt, Mol. Phys. 111, 3618 (2013)

use "narrow" semiclassical GWPs:

$$g_{\varepsilon,j_\kappa}^{(\kappa)}(r_\kappa) = N_\varepsilon \exp\left[-\frac{1}{2\varepsilon}(r_\kappa - q_{j_\kappa})\cdot a(r_\kappa - q_{j_\kappa}) + \frac{i}{\varepsilon} p_{j_\kappa}^{(\kappa)}(t)\cdot(r_\kappa - q_{j_\kappa})\right]$$

Classical Limit as Scaling Limit

- condition for classicality:

  $\lambda_{dB} \ll L$

  λ_{dB} = de Broglie wave length; L = scale of variation of the potential V
- rescale potential: $V^{\varepsilon}(r) := V(\varepsilon r)$ such that $\varepsilon \to 0$ corresponds to the limit of slow variation of V^{ε}
- switch to macroscopic coordinates: $(\tilde{r}, \tilde{t}) = (\varepsilon r, \varepsilon t)$ such that the Schrödinger Equation reads ($\hbar = 1$, $m = 1$):

$$i\varepsilon \frac{\partial}{\partial \tilde{t}} \Psi(\tilde{r}, \tilde{t}) = \left[-\frac{\varepsilon^2}{2} \Delta_{\tilde{r}} + V(\tilde{r}) \right] \Psi(\tilde{r}, \tilde{t})$$

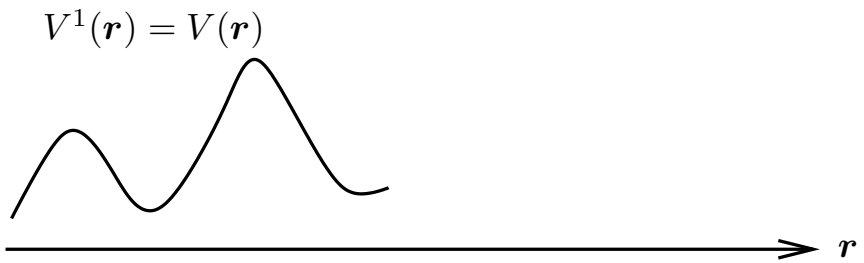

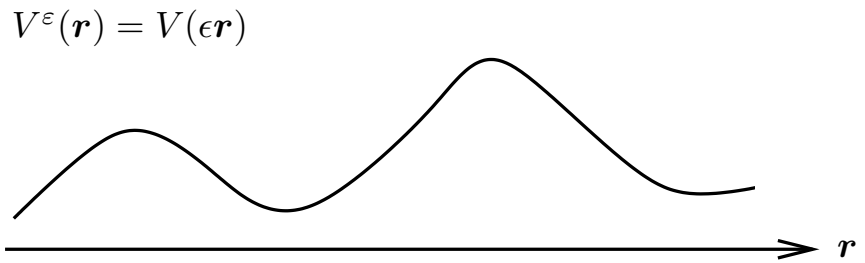

Classical-Limit Gaussian Wavepackets

$$g_{\varepsilon,j}(\tilde{r}) = N_\varepsilon \exp\left[-\frac{1}{2\varepsilon}(\tilde{r}-q_j)\cdot a(\tilde{r}-q_j) + \frac{i}{\varepsilon}p_j\cdot(\tilde{r}-q_j)\right]$$

- "narrow" wavepackets centered around position and momentum (q_j, p_j),
  $\|(\hat{r}-q_j)g_{\varepsilon,j}\| \sim \sqrt{\varepsilon} \qquad \|(\hat{p}-p_j)g_{\varepsilon,j}\| \sim \sqrt{\varepsilon}$
- move along classical trajectories (up to an error of order $\sqrt{\varepsilon}$)
  $g_{\varepsilon,j}(\tilde{r},\tilde{t}) \sim \exp\left(\frac{i}{\varepsilon}S^{\mathrm{cl}}(\tilde{t})\right) g_{\varepsilon,j}(\tilde{r}, q_j^{\mathrm{cl}}(\tilde{t}), p_j^{\mathrm{cl}}(\tilde{t}))$
- in this limit, the Gaussian wavepackets are decoupled from each other

G. Hagedorn, Ann. Inst. H. Poincaré Phys. Théor. **42** (1985), no. 4, 363, G. Hagedorn, Ann. Physics **269** (1998), 77

Mixed Quantum-Classically Evolved Wavefunction

$$\Psi^{\mathrm{qc}}(r,t) = \sum_{j_1} \cdots \sum_{j_M} \sum_{l} A^{\mathrm{qc}}_{j_1 \cdots j_M, l} \left(\prod_{\kappa=1}^{M} \varphi^{(\kappa)}_{j_\kappa}(r_\kappa, t) \right) \exp\left(\frac{i}{\varepsilon} S^{\mathrm{cl}}_l \right) g^{(f)}_{\varepsilon,l}(r_f; q^{(f)}_l, p^{(f)}_l)$$

coefficients: $i\dot{A}_l = H A_l$

SPFs (primary modes): $i\dot{\varphi}^{(\kappa)} = \left(\hat{1} - \hat{P}^{(\kappa)} \right) \left[\rho^{(\kappa)} \right]^{-1} \hat{H}^{(\kappa)} \varphi^{(\kappa)}$

classical secondary modes: $\dot{q}^{(f)}_l = p^{(f)}_l \qquad \dot{p}^{(f)}_l = -\nabla_{q_l} H^{(f)}_l$

- the resulting quantum-classical dynamics corresponds to a multiconfigurational Ehrenfest (MCE) approach
- the trajectories are still coupled through the primary-mode mean fields

Römer, Burghardt, Mol. Phys. 111, 3618 (2013)

MCE Nonadiabatic Dynamics (Diabatic Representation)

$$\hat{H} = -\frac{\varepsilon^2}{2}\nabla_r^2 \hat{1} + \hat{V} \qquad \hat{V}(r) = \begin{pmatrix} V_{11}(r) & V_{12}(r) \\ V_{12}(r) & V_{22}(r) \end{pmatrix}$$

$$|\Psi^{\mathrm{qc}}(r,t)\rangle = \sum_{n=1}^{n_{\mathrm{states}}} \sum_{l=1}^{n_G} A_{nl}(t) \exp\left(\frac{i}{\varepsilon} S_l^{\mathrm{cl}}(t)\right) g_{\varepsilon,l}(r; q_l(t), p_l(t)) \, |n\rangle \qquad (\text{“single-set”})$$

coefficients: $i\dot{\boldsymbol{A}}_l = \boldsymbol{H}(q_l)\boldsymbol{A}_l$

classical modes: $\dot{q}_l = p_l \qquad \dot{p}_l = -\nabla_{q_l} \bar{V}_l(q_l)$

with the mean-field potential $\bar{V}_l = \left[\sum_n |A_{nl}|^2\right]^{-1} \sum_n \sum_{n'} A_{nl}^* A_{n'l} \langle n|\hat{V}(r = q_l)|n'\rangle$

- Ψ^{qc} evolves along a superposition of Ehrenfest trajectories
- similarly for adiabatic representation (kinetic energy couplings)

see also Shalashilin, J. Chem. Phys. 130, 244101 (2009), 132, 244111 (2010)

Ehrenfest & Beyond

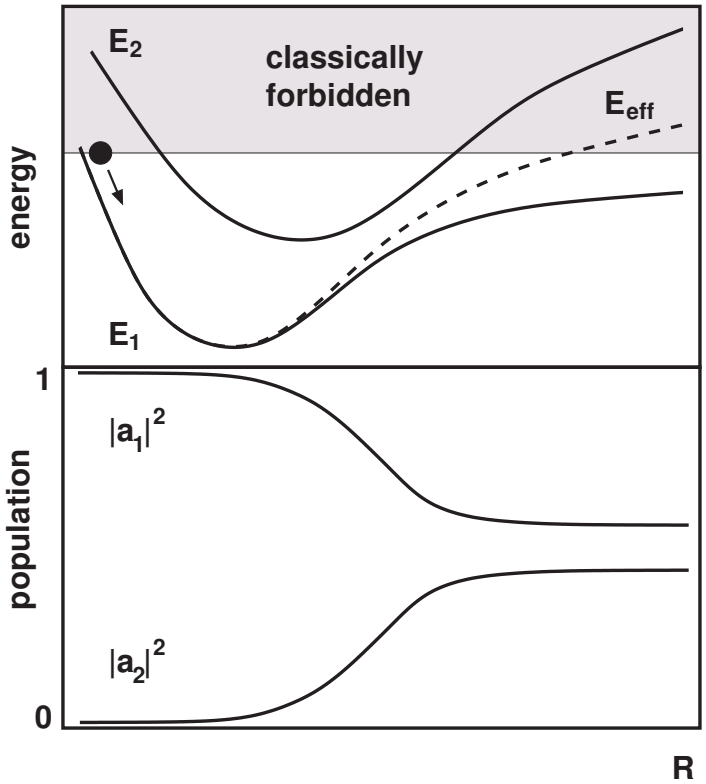

N. L. Doltsinis, in: Quantum Simulations of Complex Many-Body Systems: From Theory to Algorithms NIC Series, Jülich, 10, p. 377 (2002)

- single Ehrenfest trajectory: mean field
  $\bar{V}(q) = \sum_{n,n'} A_n A_{n'} \langle n|\hat{V}(q)|n'\rangle$

  Delos, Thorson, Knudson, Phys. Rev. A 6, 709 (1972)
  Billing, Chem. Phys. Lett. 100, 535 (1983)

- multiconfigurational Ehrenfest: coherent superposition of trajectories (q_l, p_l) with mean fields
  $\bar{V}_l(q_l) = [\sum_n |A_{nl}|^2]^{-1} \sum_{n,n'} A^*_{nl} A_{n'l} \langle n|\hat{V}(q_l)|n'\rangle$

  Shalashilin, J. Chem. Phys. 130, 244101 (2009), 132, 244111 (2010)
  Römer, Burghardt, Mol. Phys. 111, 3618 (2013)

- different from statistical Ehrenfest approach

  Alonso et al., J. Chem. Phys. 137, 054106 (2012)

MCE-like Dynamics for Non-Scaled GWPs

- important in practice, in view of GWP-based sampling of initial conditions and guaranteeing norm conservation
- two-layer ansatz required to restrict electronic coupling to lth subspace:

$$|\Psi^{\mathrm{qc}}(r,t)\rangle = \sum_{l=1}^{n_G} \tilde{A}_l(t)|\Phi_l^{\mathrm{qc}}(r,t)\rangle = \sum_{l=1}^{n_G} \tilde{A}_l(t)\exp\left(\frac{i}{\hbar}S_l^{\mathrm{cl}}(t)\right) g_l(r;q_l(t),p_l(t))\,|\chi_l^{(\mathrm{el})}(t)\rangle$$

$$|\chi_l^{(\mathrm{el})}(t)\rangle = \sum_{n=1}^{n_{\mathrm{states}}} B_{nl}(t)|n\rangle$$

$\tilde{\boldsymbol{A}}$ coefficients: $i\boldsymbol{S}\dot{\tilde{\boldsymbol{A}}} = (\boldsymbol{H} - i\tau)\tilde{\boldsymbol{A}}$

$\boldsymbol{B}$ coefficients: $i\dot{\boldsymbol{B}}_l = \boldsymbol{H}(q_l)\boldsymbol{B}_l$

classical modes: $\dot{q}_l = p_l \quad \dot{p}_l = -\nabla_{q_l}\bar{V}_l(q_l)$

with the mean-field potential $\bar{V}_l = \left[\sum_n |B_{nl}|^2\right]^{-1} \sum_n \sum_{n'} B_{nl}^* B_{n'l} \langle n|\hat{V}(r=q_l)|n'\rangle$

see also Shalashilin, J. Chem. Phys. 132, 244111 (2010)

Multiconfigurational Ehrenfest Dynamics

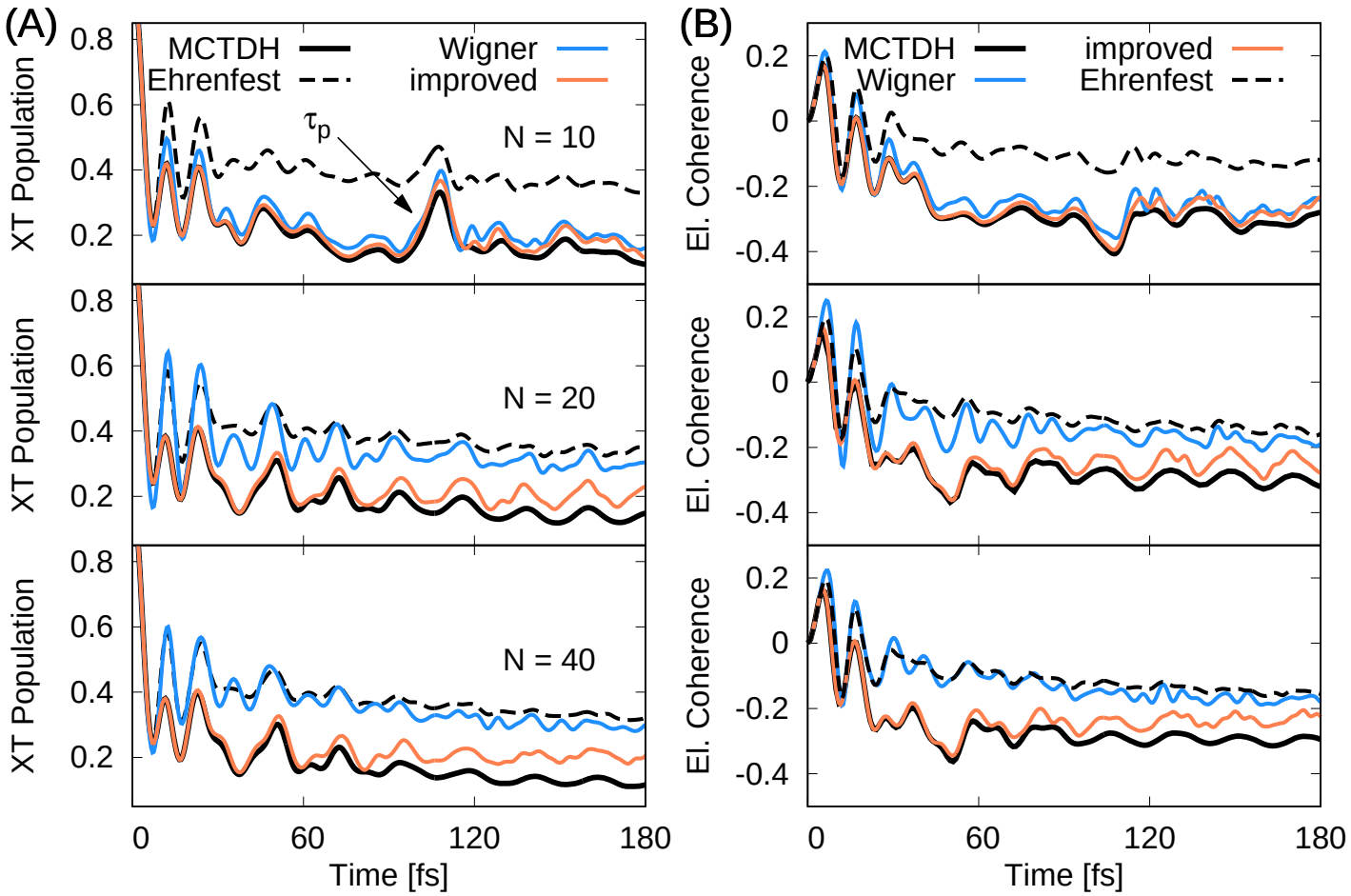

- 2000 MCE configurations vs. 5000 statistical Ehrenfest trajectories
- convergence for Wigner sampling quite good up to $N = 10$ modes
- beyond $N = 10$, improved sampling (notably compression) becomes crucial

Multiconfigurational Ehrenfest System – Properties

- the quantum-classical wavefunction state carries correlations due to the multiconfigurational wavefunction form,

$$\Psi^{\mathrm{qc}}(r,t) = \sum_J \sum_l A^{\mathrm{qc}}_{J,l}(t)\Phi_J(r_\kappa,t)\exp\left(\frac{i}{\varepsilon}S^{\mathrm{cl}}_l\right) g^{(f)}_{\varepsilon,l}(r_f;q^{(f)}_l,p^{(f)}_l)$$

- the reduced density matrix of the quantum subsystem is in a mixed state,[3]

$$\rho^{sys}_{qc}(x,x',t) = \mathrm{Tr}_{cl}\left[\Psi^{\varepsilon}_{qc}(x,r,t)\Psi^{\varepsilon *}_{qc}(x',r',t)\right]$$

- statistical ensembles can be constructed as follows:

$$\rho^{\varepsilon}_{qc}(x,r,x',r',t) = \sum_n p_n \Psi^{\varepsilon}_{qc,n}(x,r,t)\Psi^{\varepsilon *}_{qc,n}(x',r',t)$$

[3] By contrast, single-trajectory Ehrenfest evolution always yields a pure subsystem state.

Is Multiconfigurational Ehrenfest Dynamics Consistent?

- the properties of the underlying wavefunction state Ψ_{qc} are preserved
- correlations between the quantum and classical subspaces are accounted for
- the dynamics is variational, hence a generalized Poisson bracket structure exists: $i\{\cdot,\cdot\}_{qc} = i\sum_n\{\langle H\rangle, A_n\} + i\sum_l\{\langle H\rangle, \xi_l\}$ where $\langle H\rangle = \langle\Psi_{qc}|\hat{H}|\Psi_{qc}\rangle$

However,

- the single-configurational (standard Ehrenfest) case is not a satisfactory quantum-classical description
- due to the non-linear structure of the equations, a direct comparison with other approaches (e.g., the QC Liouville Equation) is not straightforward

Summary

- G-MCTDH/ML-G-MCTDH/vMCG are useful due to their proximity to classical mechanics, while permitting full quantum convergence
- two-layer (or multi-layer) variant employs correlated FG-based particles; need for sampling strategies when combining with on-the-fly applications
- natural quantum-classical limit of G-MCTDH: multiconfiguration Ehrenfest
- perspective:
  - direct dynamics combined with 2L-GMCTDH (*via* neural network fits)
  - statistical sampling & extension to thermal GWPs
  - GWP-based correlation functions
  - GWP calculations for nonlinear optical signals
  - transport dynamics
  - multiscale microscopic/mesoscopic dynamics

Acknowledgments & Collaborations

Group Frankfurt:

- M. Biswas
- P. Mondal
- D. Rastädter
- R. Binder
- J. Wahl
- P. Eisenbrandt
- M. Polkehn
- M. Huix-Rotllant

Former members:

- S. Römer
- M. Ruckenbauer
- J. Ortiz-Sánchez

Collaborations:

- H. Tamura (Sendai, Japan)
- K. H. Hughes (Bangor, UK)
- R. Martinazzo (Milano, Italy)
- H. Lischka, A. Aquino (TTU, USA)
- F. Plasser (Heidelberg, Germany)
- J. Wenzel, A. Dreuw (Heidelberg, Germany)
- S. Haacke, S. Méry (Strasbourg, France)
- F. Sterpone (IBPC, Paris)
- E. R. Bittner (Houston University, USA)
- L. S. Cederbaum (Heidelberg, Germany)
- A. Panda (IIT Guwahati, India)
- D. Beljonne, Y. Olivier (Mons, Belgium)

Thanks to: DFG, CNRS, ANR (France) for financial support

cost EUROPEAN COOPERATION IN SCIENCE AND TECHNOLOGY
MPNS COST Action MP1006

CLiC

GOETHE UNIVERSITÄT FRANKFURT AM MAIN

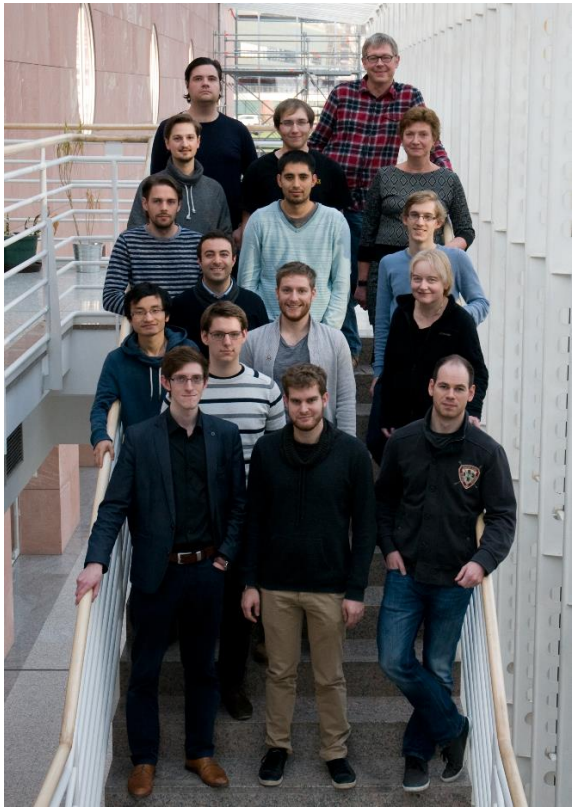

Theoretical Chemistry
of Complex Systems

AK Burghardt

Quantum Coherence Plays a Non-Negligible Role!

$$|\psi(t)\rangle = c_0(t)|0\rangle|\phi_0(t)\rangle + c_1(t)|1\rangle|\phi_1(t)\rangle$$

electronic coherence:

$$\rho_{01}(t) = \mathrm{Tr}[|0\rangle\langle 1|\hat{\rho}(t)]$$
$$= \langle 1|\hat{\rho}(t)|0\rangle = c_1^*(t)c_0(t)\langle\phi_1(t)|\phi_0(t)\rangle$$

- coherence $\propto$ overlap of nuclear wavefunctions
- typical decoherence times: tens to hundreds of fs or more (estimate from $\tau_{\mathrm{dec}} \sim \tau_g(6k_BT/\lambda)^{1/2}$ or $\tau_{\mathrm{dec}} \sim \gamma^{-1}(\lambda_T/\Delta x)^2)$

  Prezdho, Rossky, PRL 81, 5294 (1998)
- loss of coherence not captured by classical trajectory picture

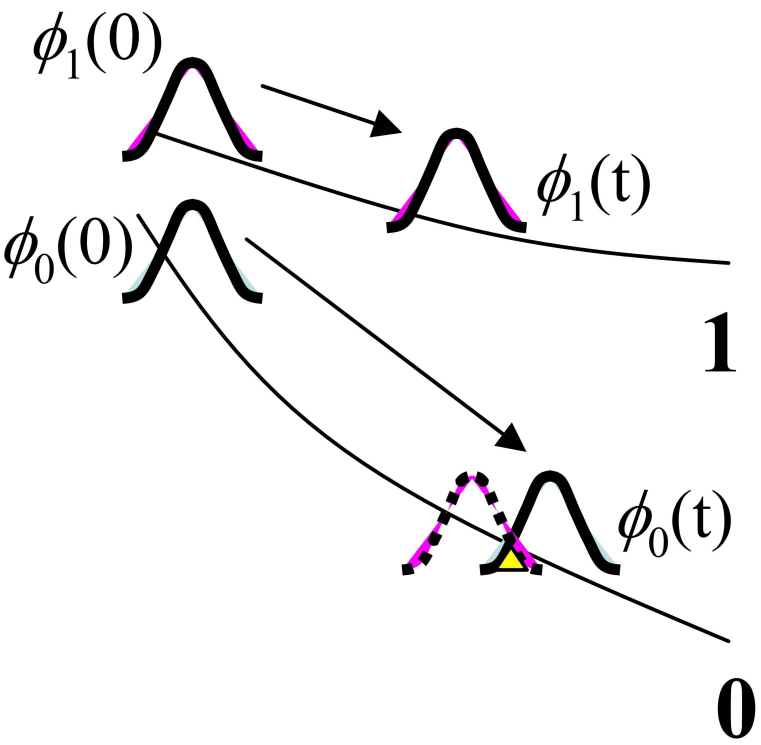

picture: P. Rossky et al.

Multiconfigurational Ehrenfest Dynamics

- 4D – 40D spin-boson system
- several 1000 trajectories
- importance sampling over ρ_{Wigner}
- strong dependence on GWP width

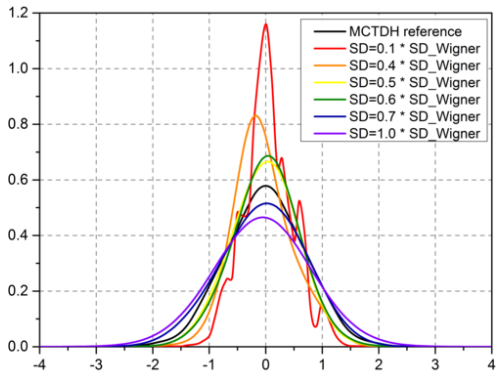

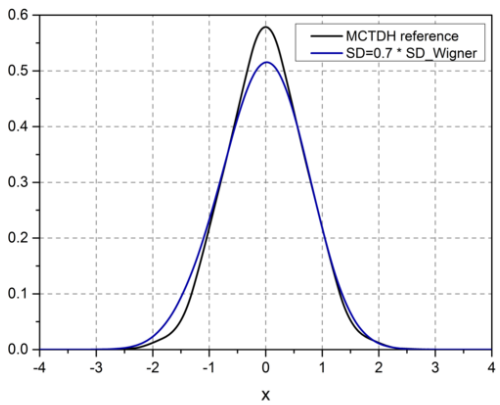

- Multiconfiguration Ehrenfest

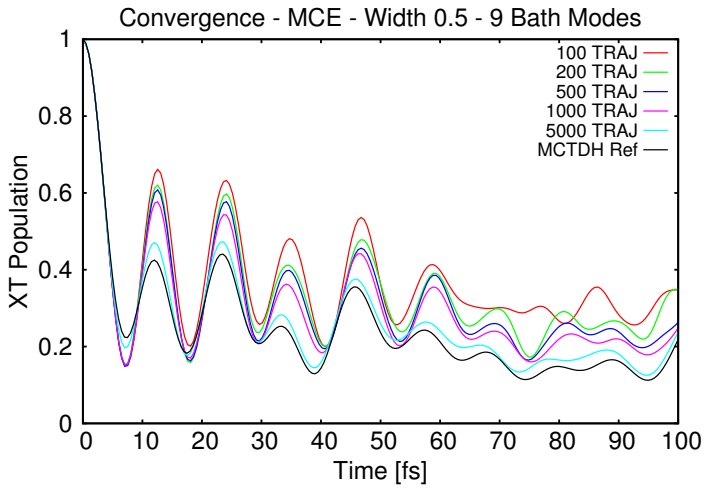

- For Comparison: Statistical Ehrenfest

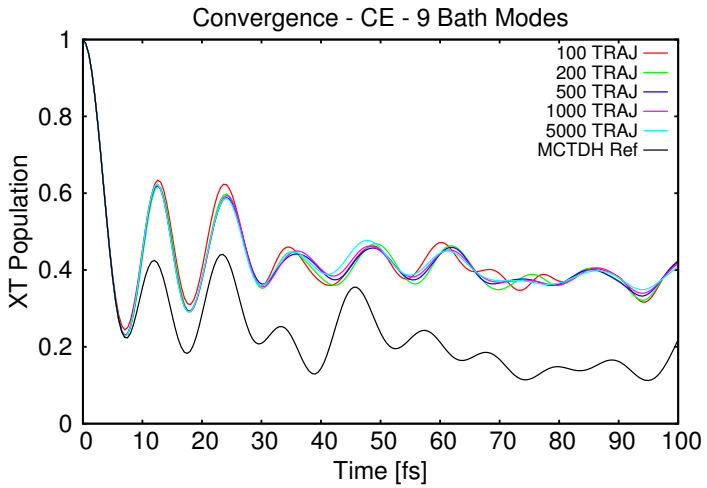

Coupled Electronic States: Single-Set, Multi-Set, Hybrid-Set

Example: 20-mode calculation for donor-acceptor system

single-set

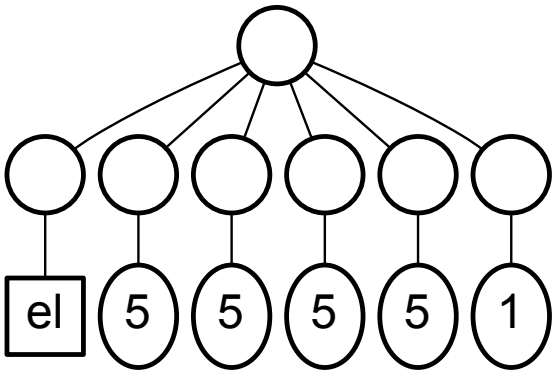

multi-set

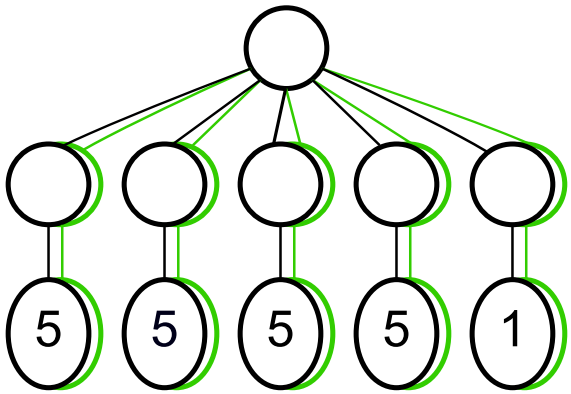

hybrid multi/single-set

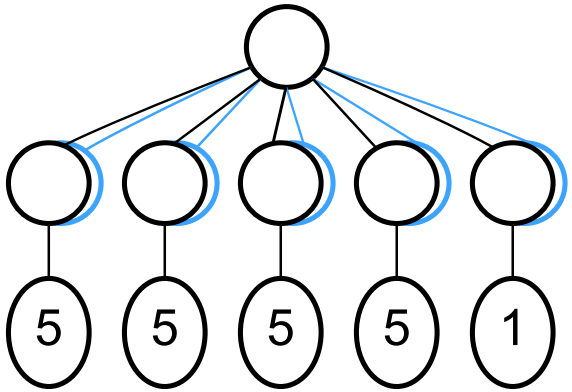

Eisenbrandt, Ruckenbauer, Burghardt, submitted (2018)

- convergence properties can differ significantly depending on the system

Model System: Intramolecular Vibrational Redistribution (IVR)

$$\hat{H} = \hat{T} + \frac{1}{2}\sum_{i=1}^{n}\sum_{j=1}^{m}\omega_i \hat{q}_{i,\,j}^2 + \frac{1}{2}\sum_{i=1}^{n-1} k\left(\hat{q}_{i,1} - \hat{q}_{i+1,1}\right)^2 + \Delta\sum_{i=1}^{n}\sum_{j=2}^{m}\hat{q}_{i,1}^2\hat{q}_{i,j}$$

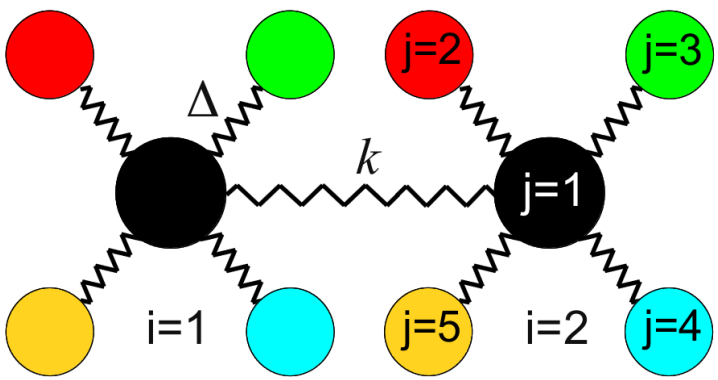

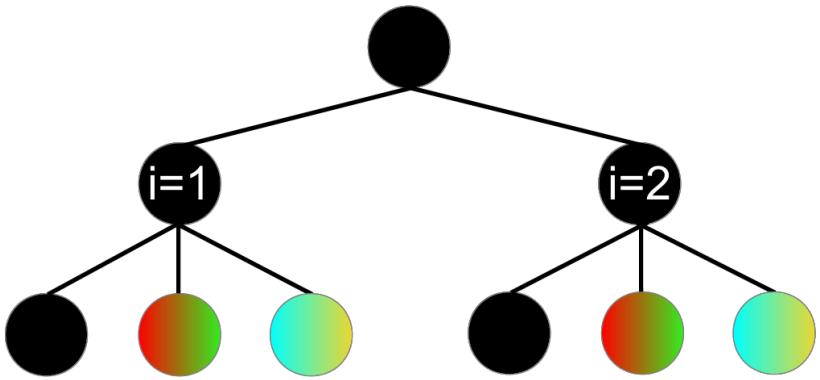

Schade, Hamm, J. Chem. Phys. **131**, 044511 (2009), Eisenbrandt, Ruckenbauer, Römer, Burghardt, to be submitted (2018)

- low-frequency transporting modes + high-frequency local modes
- transporting/local modes communicate via Fermi resonances
- IVR efficiency is controlled by parameters k and Δ
- consider regime of "ballistic" transport along the chain
- $i = 1, \ldots f_1$ 1st-layer modes , $j = 1, \ldots f_2$ 2nd-layer modes/site

Model System: PES Cuts

$$\hat{H} = \hat{T} + \frac{1}{2}\sum_{i=1}^{n}\sum_{j=1}^{m}\omega_i \hat{q}_{i,\,j}^2 + \frac{1}{2}\sum_{i=1}^{n-1} k\left(\hat{q}_{i,1} - \hat{q}_{i+1,1}\right)^2 + \Delta\sum_{i=1}^{n}\sum_{j=2}^{m}\hat{q}_{i,1}^2\hat{q}_{i,j}$$

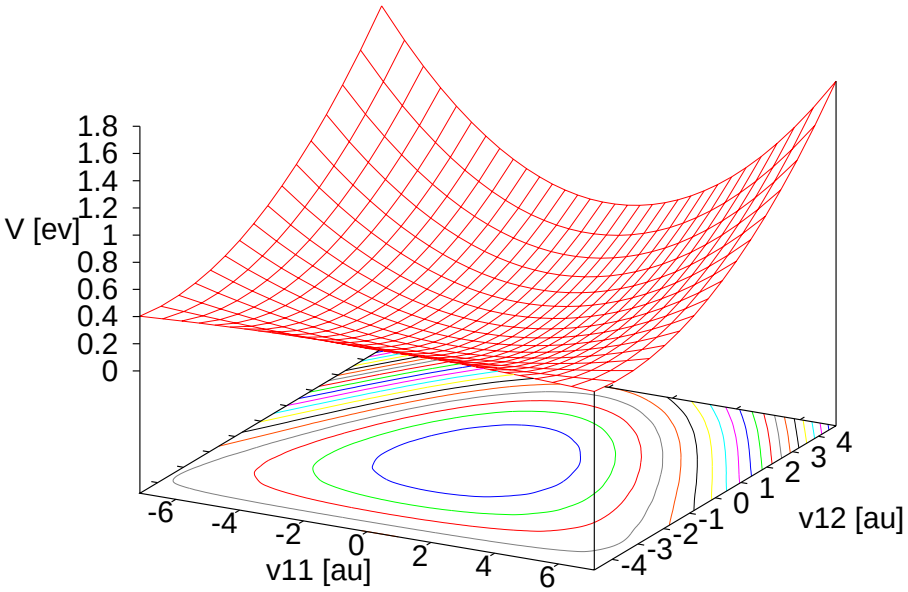

intra-site PES cut (q_{11}, q_{12})

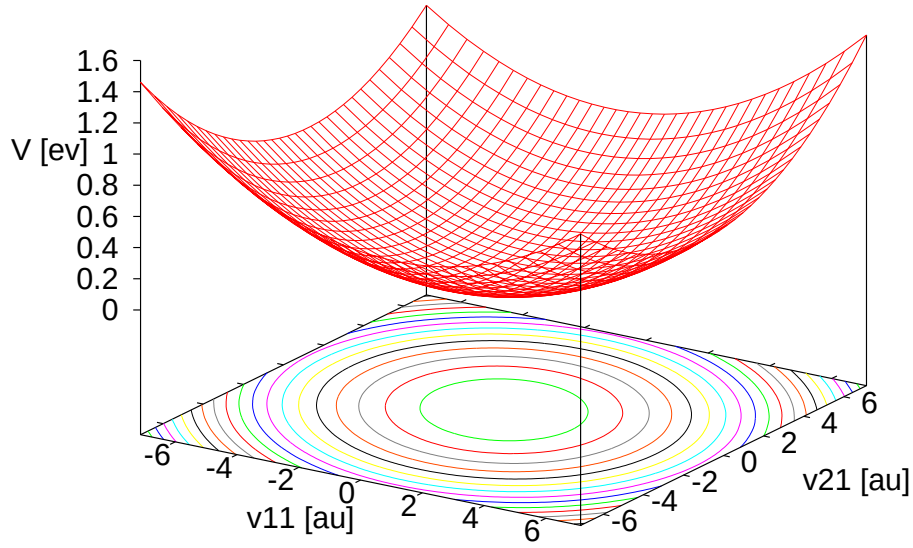

PES cut for transporting modes (q_{11}, q_{21})

Results & Benchmarks

18 sites
90 DOFs
1st/2nd layer modes:
$f_1 = 6, f_2 = 6$
1st/2nd layer SPFs:
$n_1 = 3, n_2 = 3$

[140 hrs/36 MB]
in-house code
(vs. [136 hrs/215 MB]
2L-MCTDH
HD package)

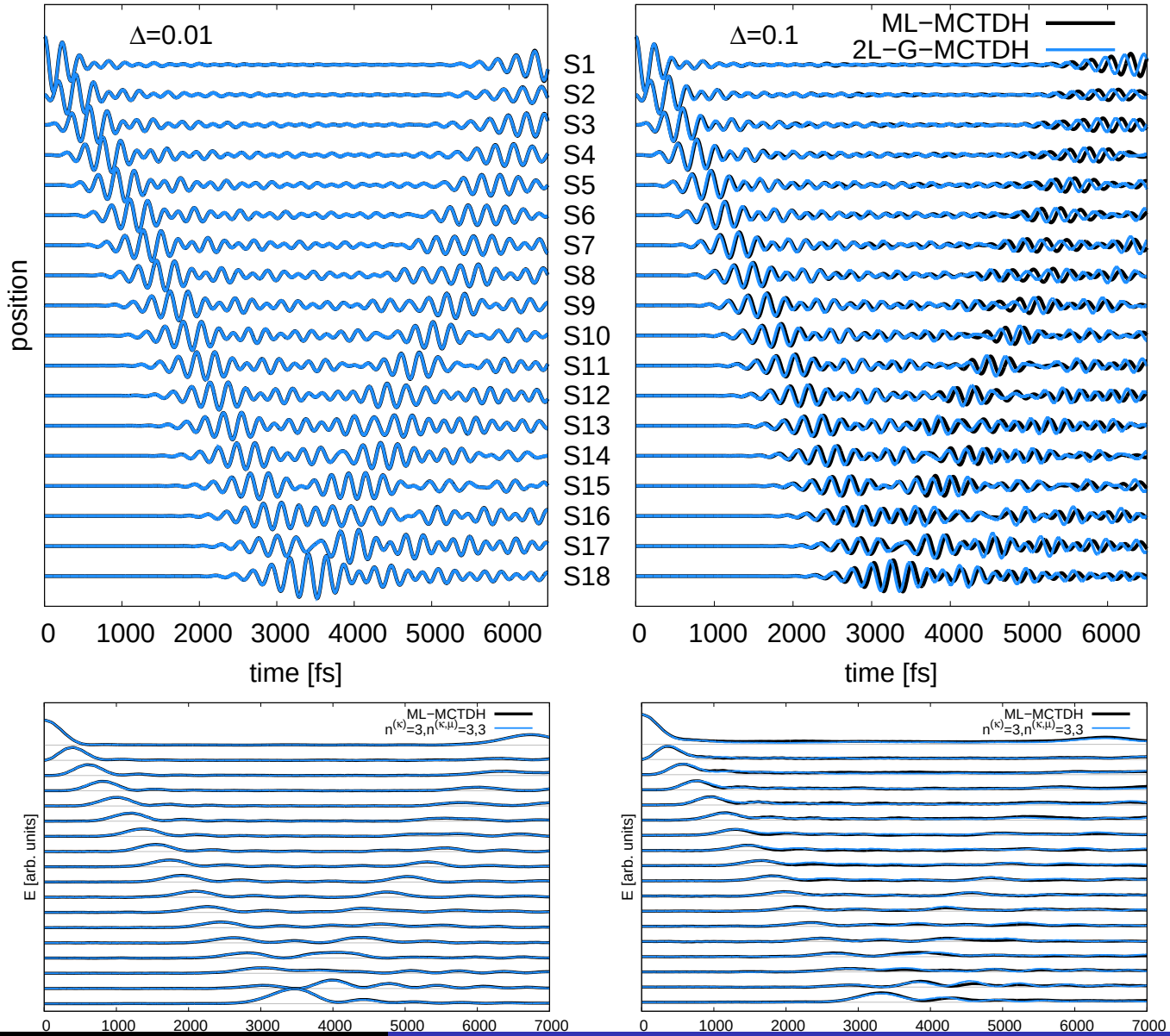

New Projector Splitting Scheme for MCTDH

concept: split subspace projectors $\mathscr{P}_\kappa = \mathscr{P}_\kappa^+(\Psi) - \mathscr{P}_\kappa^-(\Psi)$ such that:

$$\mathscr{P}(\Psi) = \mathscr{P}_0(\Psi) + \sum_\kappa \left(\mathscr{P}_\kappa^+(\Psi) - \mathscr{P}_\kappa^-(\Psi) \right)$$

where

$$\mathscr{P}_0(\Psi) = \sum_J |\Phi_J\rangle\langle\Phi_J| \quad \text{and} \quad \mathscr{P}_\kappa^+(\Psi) = \bar{P}^{(\kappa)} \qquad \mathscr{P}_\kappa^-(\Psi) = P^{(\kappa)} \otimes \bar{P}^{(\kappa)}$$

$P^{(\kappa)} = \sum_i |\varphi_i^{(\kappa)}\rangle\langle\varphi_i^{(\kappa)}|$: SPF subspace projector

$$\bar{P}^{(\kappa)} = \sum_{l,l'} |\Psi_{l'}^{(\kappa)}\rangle \, (\rho^{(\kappa)})^{-1}_{l'l} \, \langle\Psi_l^{(\kappa)}| = \sum_l |\tilde{\Psi}_l^{(\kappa)}\rangle\langle\tilde{\Psi}_l^{(\kappa)}|$$

- use a complementary representation where the SHFs are orthogonal
- two sets of coupled EoMs for SPFs where $[\rho^{(\kappa)}]^{-1}$ does not appear!

Lubich, Appl. Math. Res. eXpress 2015, 311 (2015), Kloss, Burghardt, Lubich, J. Chem. Phys., 146, 174107 (2017)
Bonfanti, Burghardt, Chem. Phys., in press (2018), arXiv:1802.01058 [physics.chem-ph]

Implementation of Projector Splitting Integrator for MCTDH

Lubich, Appl. Math. Res. eXpress 2015, 311 (2015), Kloss, Burghardt, Lubich, J. Chem. Phys. 146, 174107 (2017).

MCTDH equations in tensor notation:

$$i\dot{C} = \sum_q a_q C \times_{n=1}^{d} \mathbf{H}^q_{spf,n} \tag{1}$$

$$\dot{\mathbf{U}}_n = \sum_q a_q \left(\mathbf{I} - \mathbf{P}_n\right) \mathbf{H}^q_{prim,n} \mathbf{U}_n \mathscr{H}^q_n \rho_n^{-1} \tag{2}$$

To obtain Lubich's projector-splitting scheme, replace (2) with the following, where $\mathbf{K}_n = \mathbf{U}_n \mathbf{S}_n$ can be understood as modified SPFs that are *not* orthonormal – while the single-hole functions (SHFs) have been orthogonalized,

$$\begin{aligned} i\dot{\mathbf{K}}_n &= \sum_q a_q \mathbf{H}^q_{prim,n} \mathbf{U}_n \mathbf{S}_n \mathscr{H}^q_n \\ i\dot{\mathbf{S}}_n &= \sum_q a_q \mathbf{H}^q_{SPF,n} \mathbf{S}_n \tilde{\mathscr{H}}^q_n \end{aligned}$$

- The inverse of the density matrix no longer appears!

Example: System-Bath Correlations and Decoherence

Thawed Gaussians (TGs)

cat state + 60 HO-bath

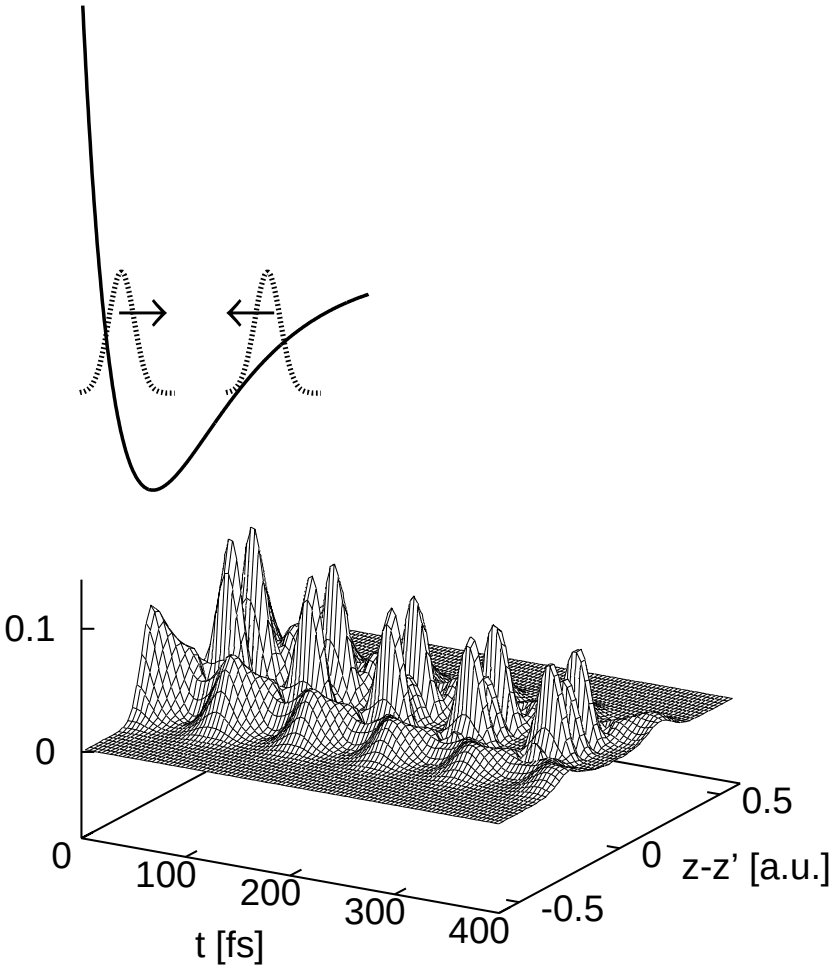

coherence $\rho(z,z')$

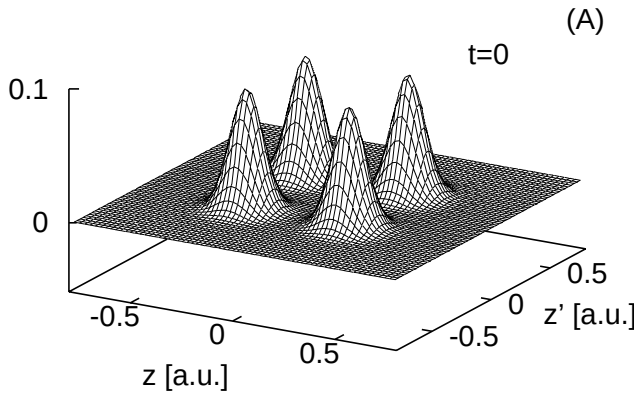

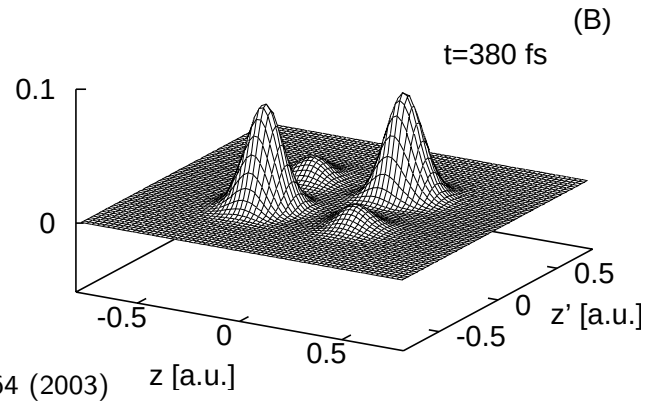

Burghardt, Nest, Worth, JCP 19, 5364 (2003)

G-MCTDH: Morse Oscillator + 60-Mode Harmonic Bath

Thawed Gaussians (TGs)

decoherence

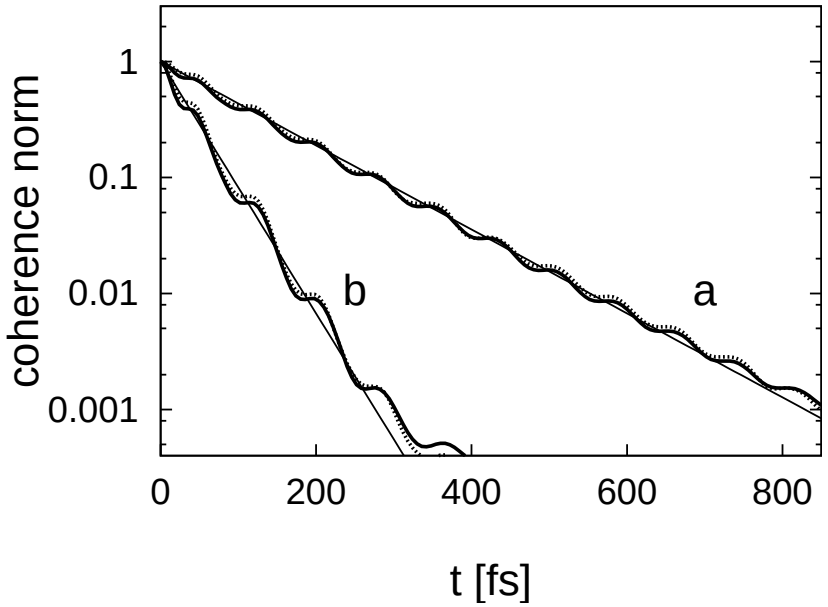

energy relaxation

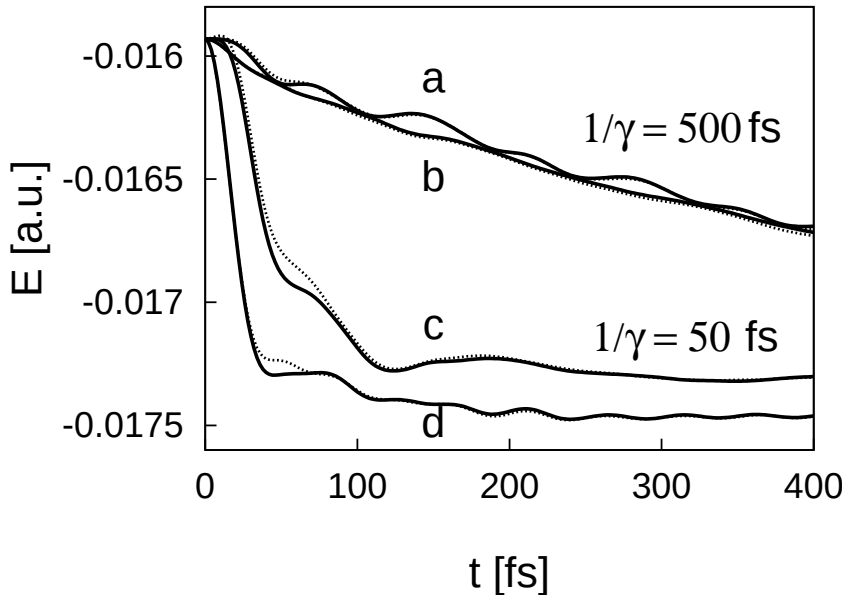

- typical configuration: $([5]_{\text{core}}, [3,3,3,4,4,3,3,3]_{\text{bath}})$

Burghardt, Nest, Worth, JCP 19, 5364 (2003)

vMCG Calculation for Herzberg-Teller Spectrum of Formaldehyde (6 dof's) (FGs)

- up to 108 GWPs
- Local Cubic Approximation
- dominant modes: out-of-plane-bending, CO stretch
- vMCG outperforms HK-SCIVR (10^5 traj.)

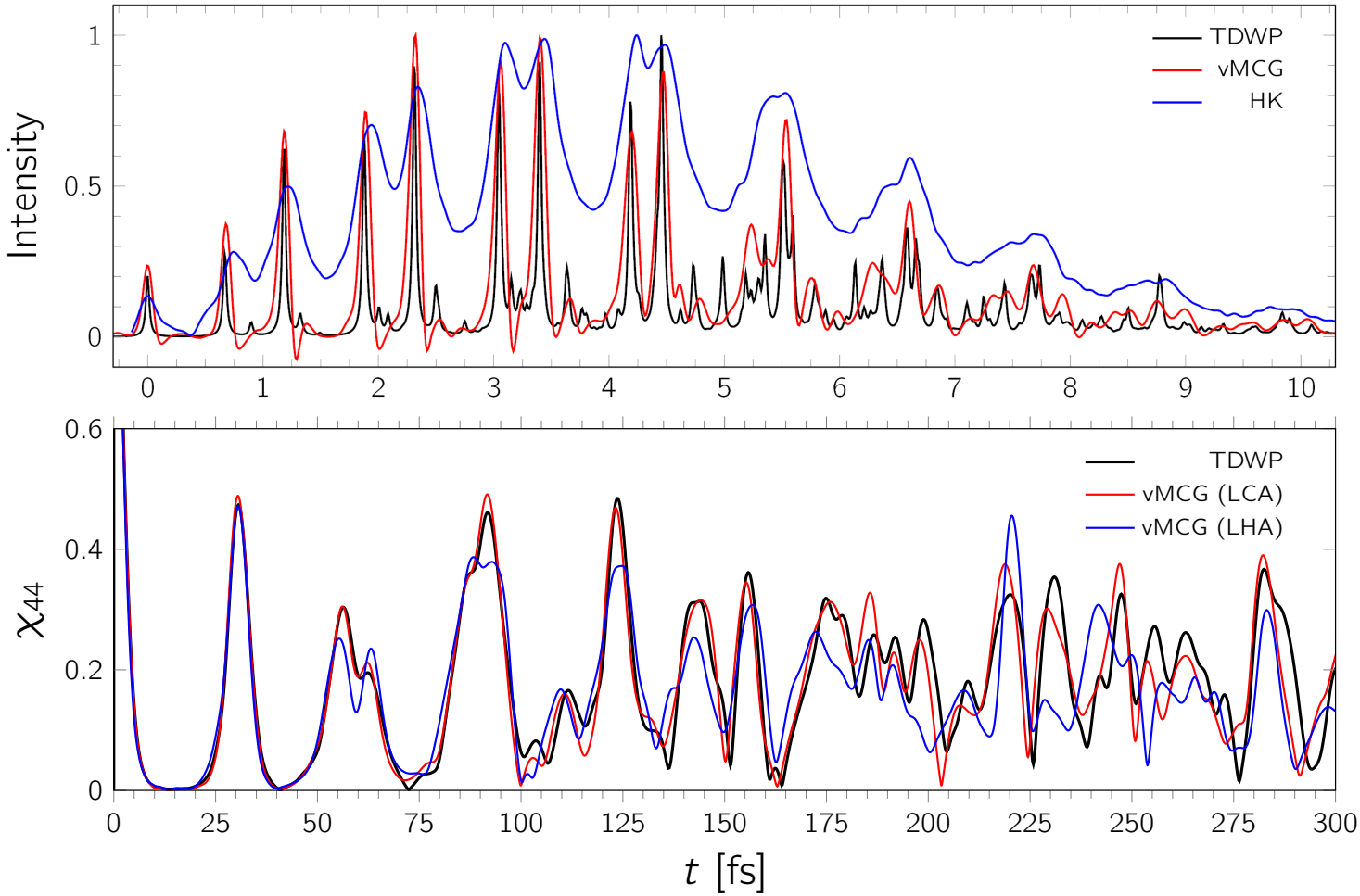

Bonfanti, Petersen, Eisenbrandt, Burghardt, Pollak, JCTC, submitted (2018).

Stochastic Schrödinger Equation in GWP/Mean-Field Setting

Burghardt, Meyer, Cederbaum, J. Chem. Phys. 111, 2927 (1999), see also: Peskin, Steinberg, J. Chem. Phys. 109, 704 (1999)

For example, consider a vMCG wavefunction + Hartree bath:

$$\psi(r_1,\ldots,r_N,\{q_n\},t) = \left[\sum_j A_j(t)\, g_j(r_1,\ldots,r_N,\Lambda(t))\right] \prod_{n=1}^{\infty} \chi^{(n)}(q_n,t)$$

Take a bath acting upon the kth DOF of the GWP particle: $\hat{H}_{SB} = -\sum_n c_{kn}\hat{r}_k\hat{q}_n$, resulting in the mean-field Hamiltonian

$$\langle H\rangle_{jl}(t) \quad = \quad -\rho_{jl}(t)\,\hat{r}_k \sum_n c_{kn}\langle\chi^{(n)}(t)|\hat{q}_n|\chi^{(n)}(t)\rangle = -\rho_{jl}(t)\,\hat{r}_k \sum_n c_{kn} Q_n(t)$$

Now use: $\lim_{n\to\infty}(\sum_n c_n Q_n(t)) = f(t) - \int_0^t dt'\,\zeta(t-t')\dot{Q}_k(t') + \zeta(0)Q_k(t)$

In the simplest case, we obtain a Langevin type equation for the GWPs:

$$\dot{q}_{j,k} \quad = \quad \frac{p_{j,k}}{m}$$

$$\dot{p}_{j,k} \quad = \quad -\left.\frac{\partial V_{\rm sys}}{\partial r_k}\right|_{r_k=q_k} + f(t) - \gamma\dot{Q}_k(t) + \zeta(0)\dot{Q}_k(0)$$

GWP/Langevin Dynamics: 2D Tunneling

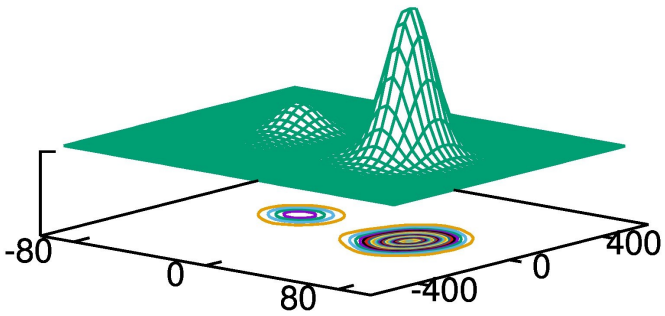

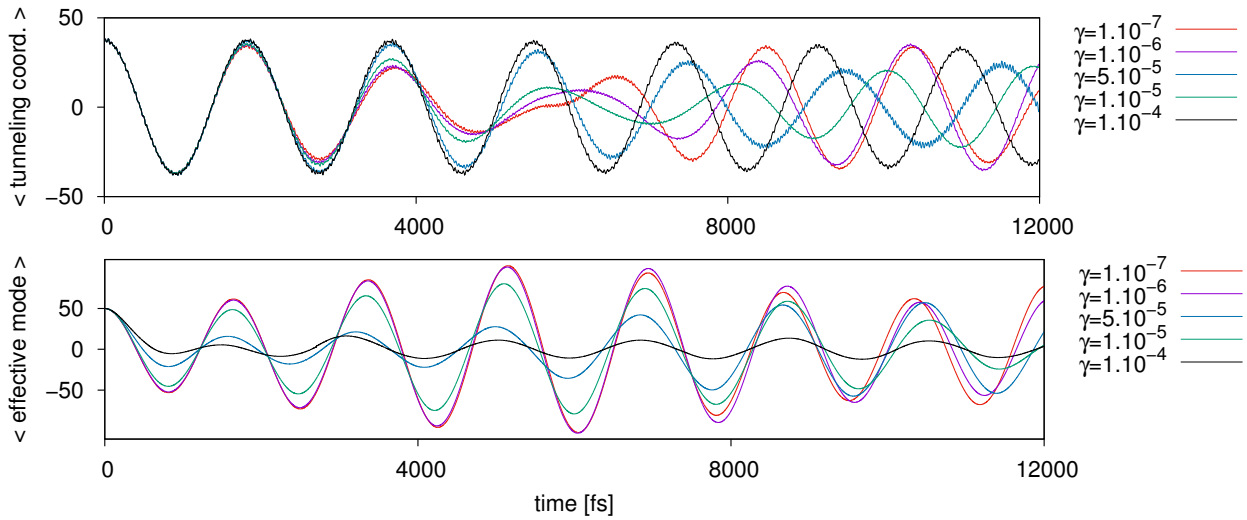

- vMCG calculations with 20 two-dimensional GWPs (not entirely converged)
- Langevin dissipation acting on harmonic coordinate
- increasing friction destroys resonant dynamics between the two modes
- general scheme: Langevin closure of effective-mode chains
- cheap and physically intuitive way of implementing dissipation

GWP/Langevin Dynamics: 2D Tunneling

tunnel coordinate $\longleftrightarrow$ $J(\omega) = \sum_n \frac{c_n^2}{\omega_n} \delta(\omega - \omega_n) = \frac{2\gamma\omega D^2}{(\Omega^2 - \omega^2)^2 + 4\gamma^2\omega^2}$

$\downarrow$

tunnel coordinate $\longleftrightarrow$ effective mode $\hat{X}_1$ $\longleftrightarrow$ $J^{\text{residual}}(\omega) = 2\gamma\omega$

- $\hat{H}_{SB} + \hat{H}_B = \hat{s} \sum_i c_n \hat{x}_n + \hat{H}_B \longrightarrow D\hat{s}\ \hat{X}_1$ – residual bath
- "Brownian oscillator" picture: 1 effective mode + Ohmic bath
- here, effective mode is chosen resonant with the tunneling frequency
- treat residual Ohmic bath by Langevin dynamics
- 2D system with damping of effective Brownian oscillator mode
- replaces discretized residual bath (or full discretization of SD)

MCTDH & G-MCTDH for Density Operators

- EOMs from variational principle for densities: $\langle\langle \delta\rho | \boldsymbol{L} - i\partial_t | \rho \rangle\rangle = 0$
- multiconfigurational density operators of two types:
  - density operators of *type I*:

$$\rho(x_1,\ldots,x_N;x'_1,\ldots,x'_N) = \sum_{\tau_1}\ldots\sum_{\tau_N} B_{\tau_1\ldots\tau_N}(t) \prod_{\kappa=1}^{N} \sigma^{(\kappa)}_{\tau_\kappa}(x_\kappa,x'_\kappa,t)$$

  - density operators of *type II*:

$$\begin{aligned}\rho(x_1,\ldots,x_N;x'_1,\ldots,x'_N) \quad = \quad & \sum_{j_1}\ldots\sum_{j_N}\sum_{l_1}\ldots\sum_{l_N} B_{j_1,\ldots,j_N;l_1,\ldots,l_N}(t) \\ & \times \prod_{\kappa=1}^{N} \varphi^{(\kappa)}_{j_\kappa}(x_\kappa,t)\,\varphi^{(\kappa)*}_{l_\kappa}(x'_\kappa,t)\end{aligned}$$

Raab, Burghardt, Meyer, J. Chem. Phys. 111, 8759 (1999), Raab, Meyer, J. Chem. Phys. 112, 10718 (2000)

- employ, e.g., in conjunction with Markovian MEs (Lindblad, Caldeira-Leggett)

G-MCTDH for Density Operators

Burghardt, Meyer, Cederbaum, J. Chem. Phys. 111, 2927 (1999)

- density operators of *type I*:

$$\rho(\boldsymbol{r};\boldsymbol{r}') = \sum_{\tau_1} \cdots \sum_{\tau_N} B_{\tau_1 \ldots \tau_N}(t) \prod_{\kappa=1}^{N} \mathscr{G}_{\tau_\kappa}^{(\kappa)}(\boldsymbol{r}_\kappa, \boldsymbol{r}'_\kappa, t)$$

$$\mathscr{G}_{\tau}^{(\kappa)}(\boldsymbol{r},\boldsymbol{r}',t) = \exp\left(\boldsymbol{r}\cdot\alpha_\tau(t)\cdot\boldsymbol{r} + \boldsymbol{r}'\cdot\alpha'_\tau(t)\cdot\boldsymbol{r}' + \beta_\tau(t)\cdot\boldsymbol{r} + \beta'_\tau(t)\cdot\boldsymbol{r}' + \boldsymbol{r}\cdot\nu'_\tau(t)\cdot\boldsymbol{r}' + \theta(t) \right)$$

- includes thermal GWPs, e.g., as initial condition:

$$\mathscr{G}_{\tau}^{(\kappa)}(r,r',t=0) = \exp\left(-\frac{m\omega}{2\sinh(\omega/kT)} \left[(r^2 + r'^2)\cosh(\omega/kT) - 2rr' \right] \right)$$

- density operators of *type II*: adjoint pairs of component densities

$$\mathscr{G}_{jl}^{(\kappa)}(\boldsymbol{r},\boldsymbol{r}',t) = g_j^{(\kappa)}(\boldsymbol{r}) g_l^{(\kappa)*}(\boldsymbol{r}') = \mathscr{G}_{lj}^{(\kappa)*}(\boldsymbol{r},\boldsymbol{r}',t)$$

Dynamics: Test Case OT-20

- Do we see trapped exciton-polarons in the dynamics?
- How exactly does the exciton migrate as the conjugation break "heals"?
- How does the spatial extension of the exciton change as a function of conformational (torsional) fluctuations?

Monomer representation:
most unbiased picture to answer these questions!

Binder, Lauvergnat, Burghardt, Phys. Rev. Lett. 120, 227401 (2018)

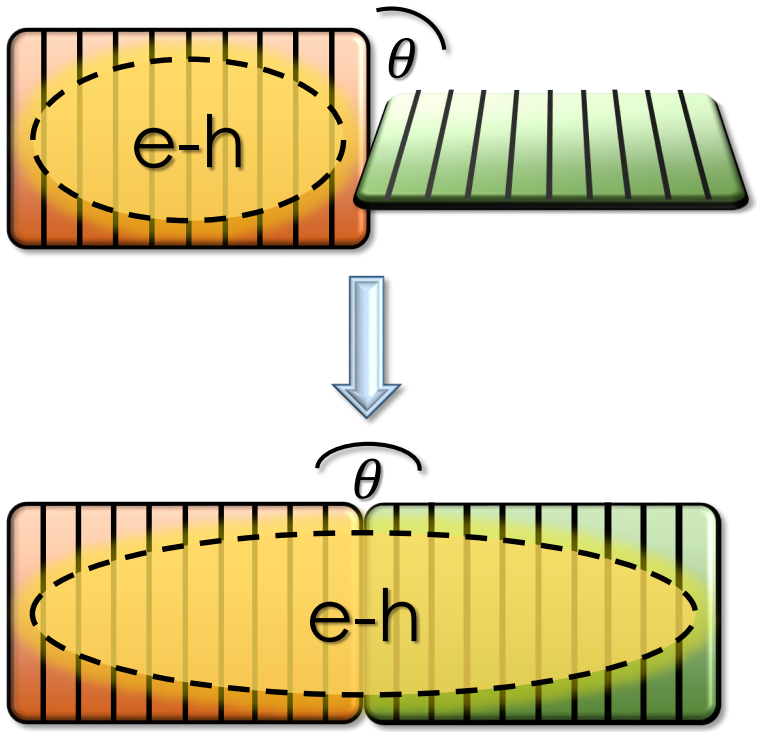

Quantum Dynamics: 20-Site J-Aggregate with Central Torsion

C-C inter-monomer mode + local C=C + torsion + bath

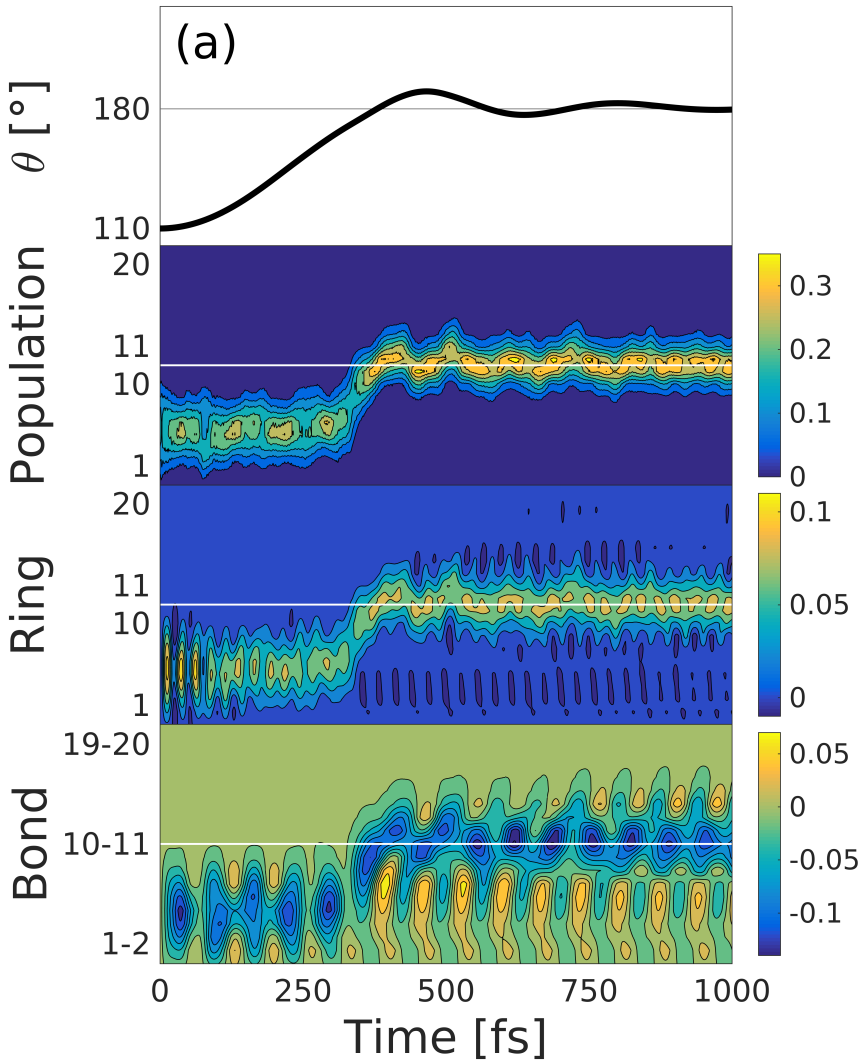

C-C inter-monomer + torsion + bath

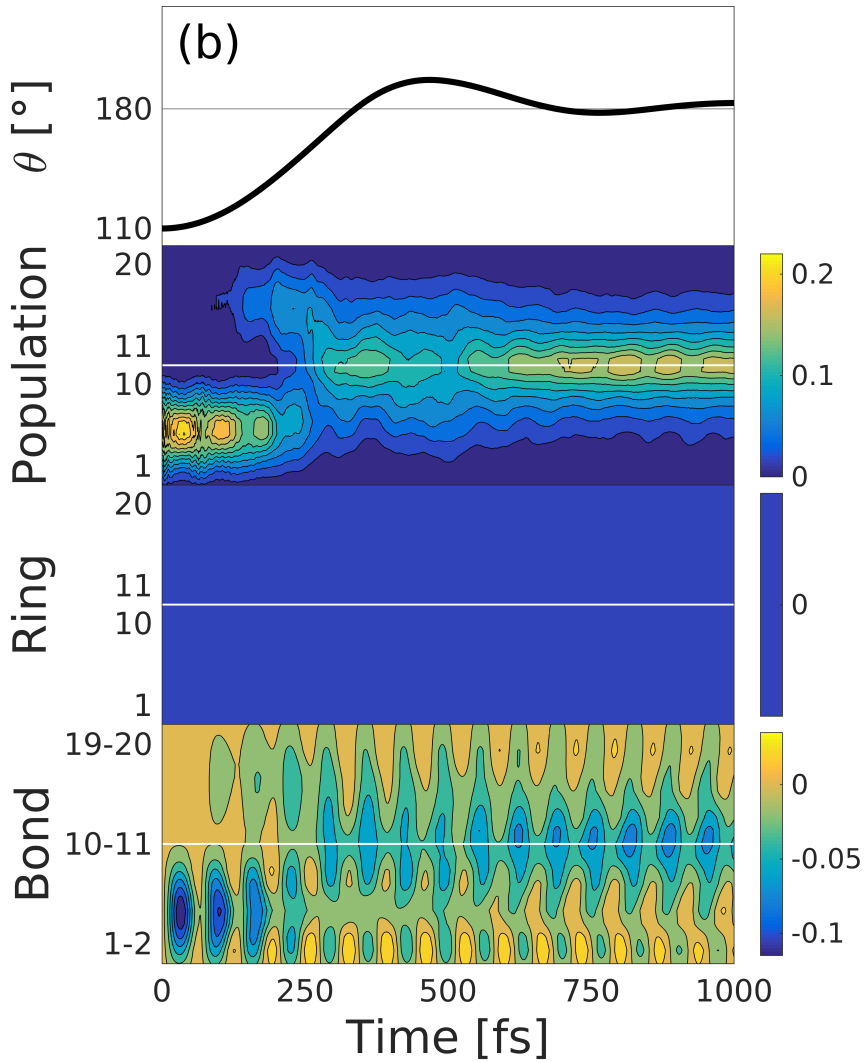

Semiclassical SQC/MM dynamics (T=0K)

SQC/MM – single trajectory

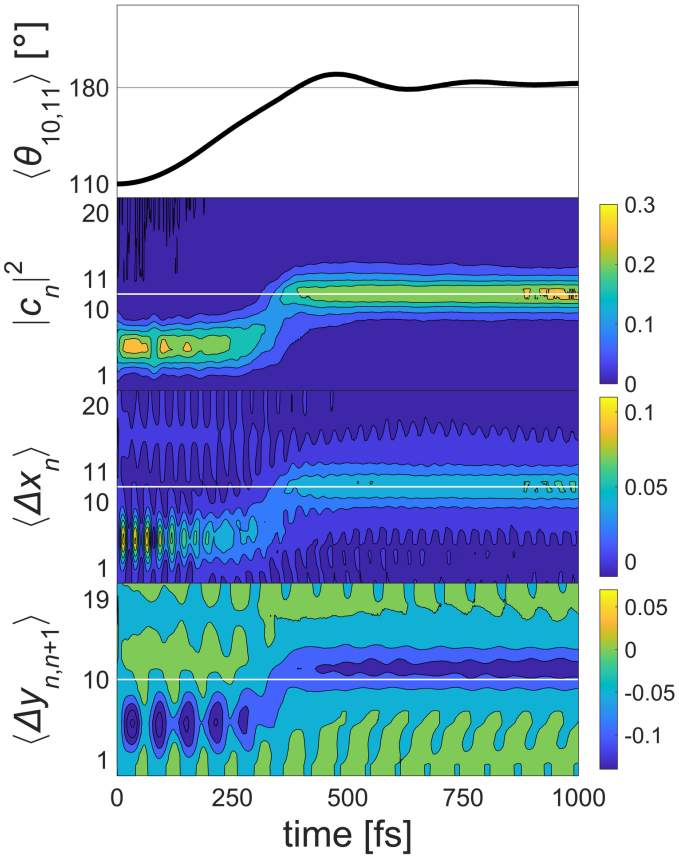

SQC/MM – Wigner average

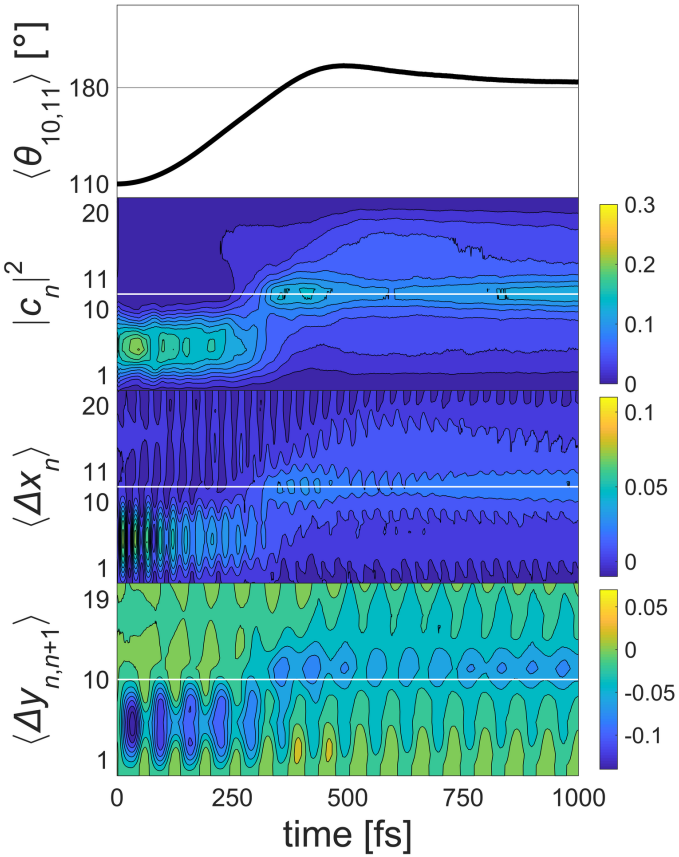

- SQC/MM = Symmetrical Quasi-Classical / Meyer-Miller model
- single-trajectory result close to MCTDH, but Wigner average "fuzzy"

Liang, Cotton, Binder, Hegger, Burghardt, Miller, J. Chem. Phys., in press (2018)

Ehrenfest/Langevin dynamics (T=0K)

Ehrenfest – single trajectory

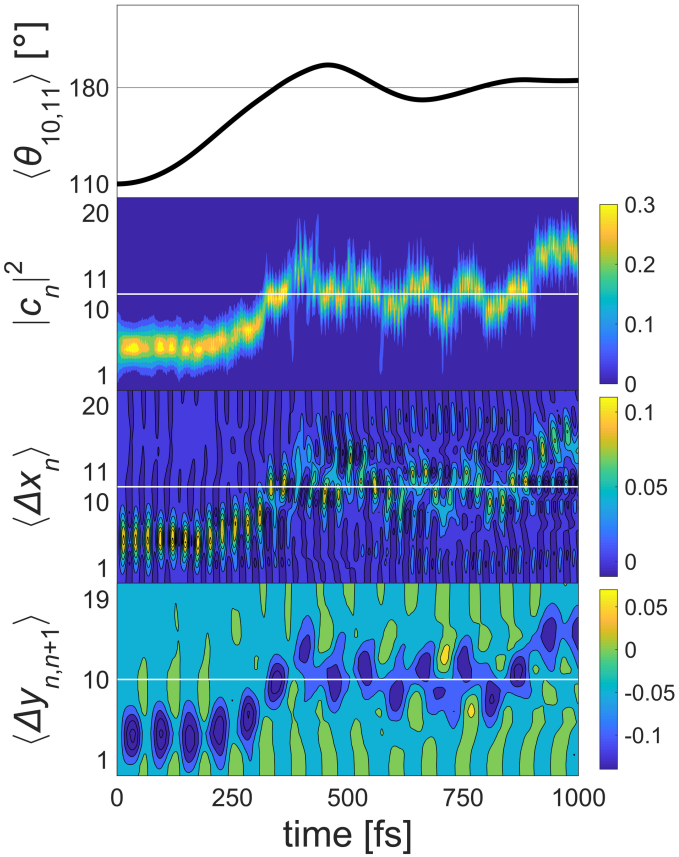

Ehrenfest – Wigner average

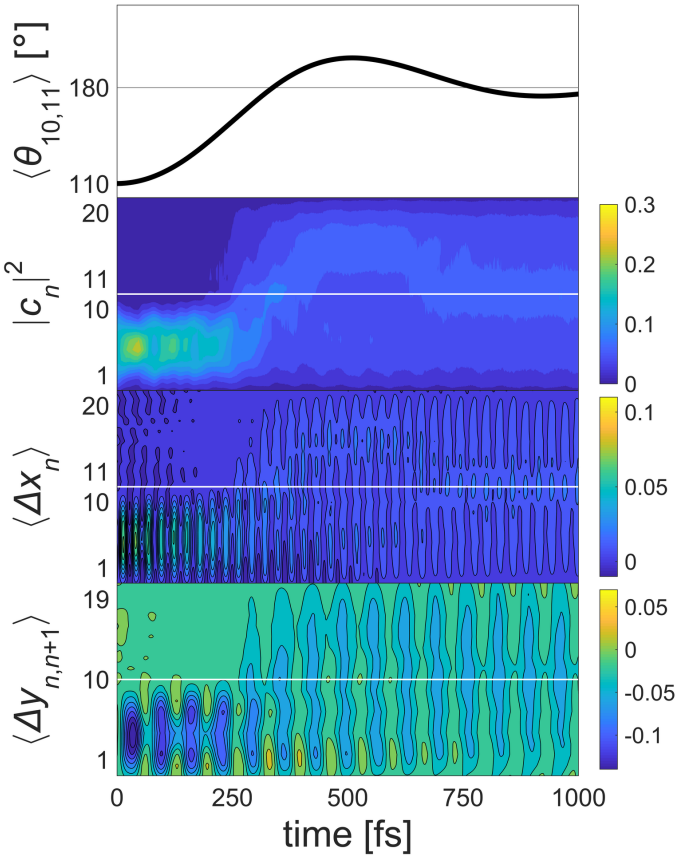

- single-trajectory dynamics exhibits fluctuations
- Wigner average "fuzzy" – due to Wigner sampling of high-frequency modes

Liang, Cotton, Binder, Hegger, Burghardt, Miller, J. Chem. Phys., in press (2018)

Adiabatic Populations (T=0K)

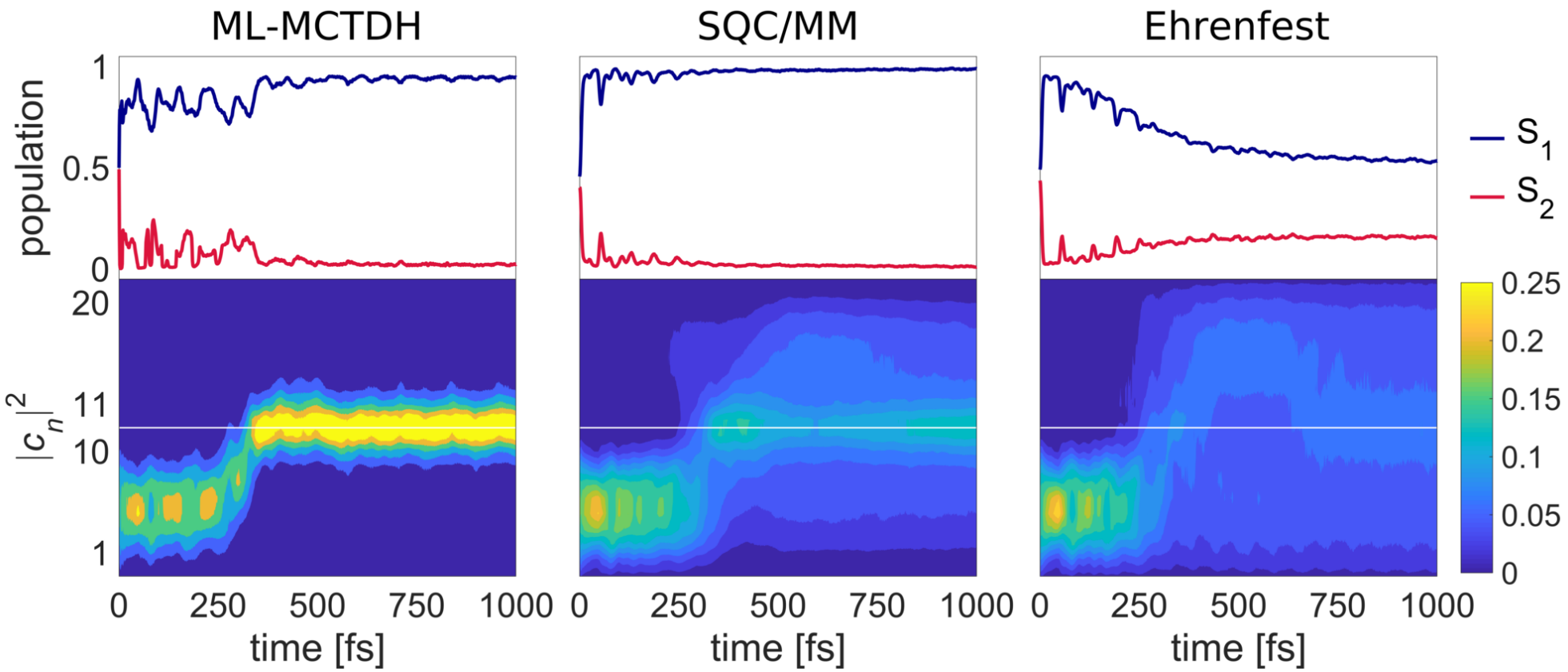

- SQC/MM reproduces the adiabatic populations quite accurately
- Ehrenfest shows severe shortcomings (related to detailed-balance problem)
- both methods incur problems due to ZPE of high-frequency modes

Liang, Cotton, Binder, Hegger, Burghardt, Miller, J. Chem. Phys., in press (2018)

Temperature Effects: Ehrenfest/Langevin dynamics

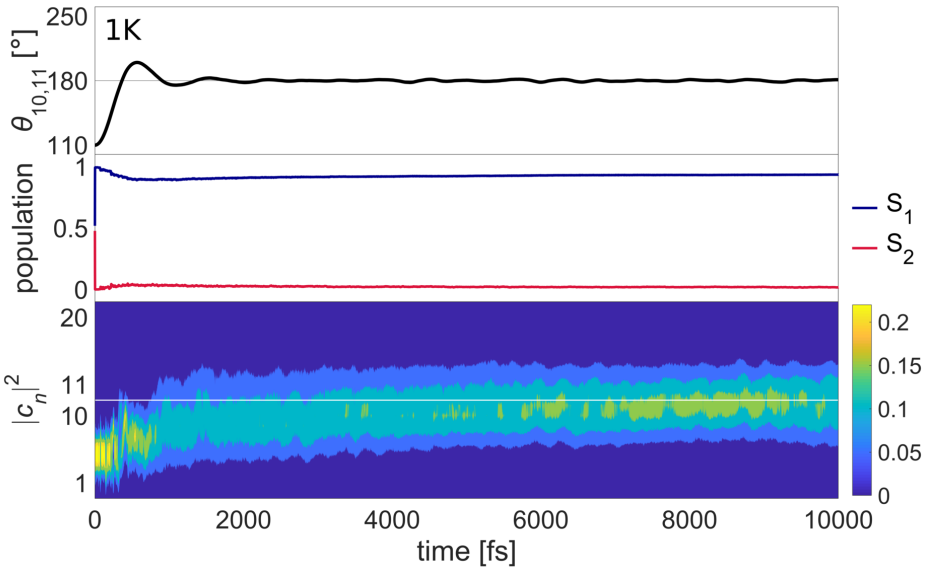

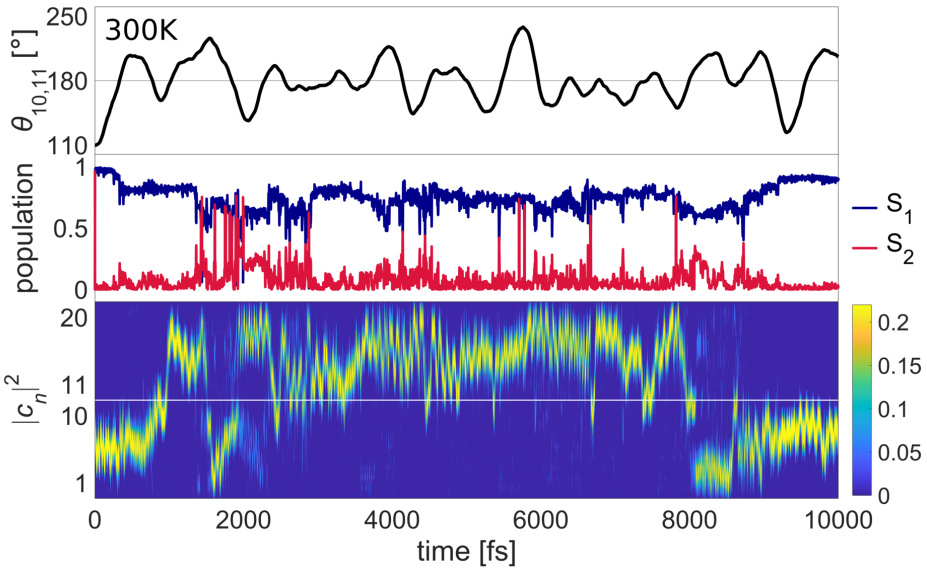

- single-trajectory simulation, with ZPE of high-frequency modes removed
- exciton migration at higher T is related to repeated non-adiabatic events
- interplay of torsional fluctuations and trapping explains observations
- quantum benchmark simulations needed (*via* random-phase wavefunctions, or thermofield method, combined with MCTDH)

Wahl, Hegger, Binder, Burghardt, in preparation

Multiconfigurational Ehrenfest Dynamics, Cont'd

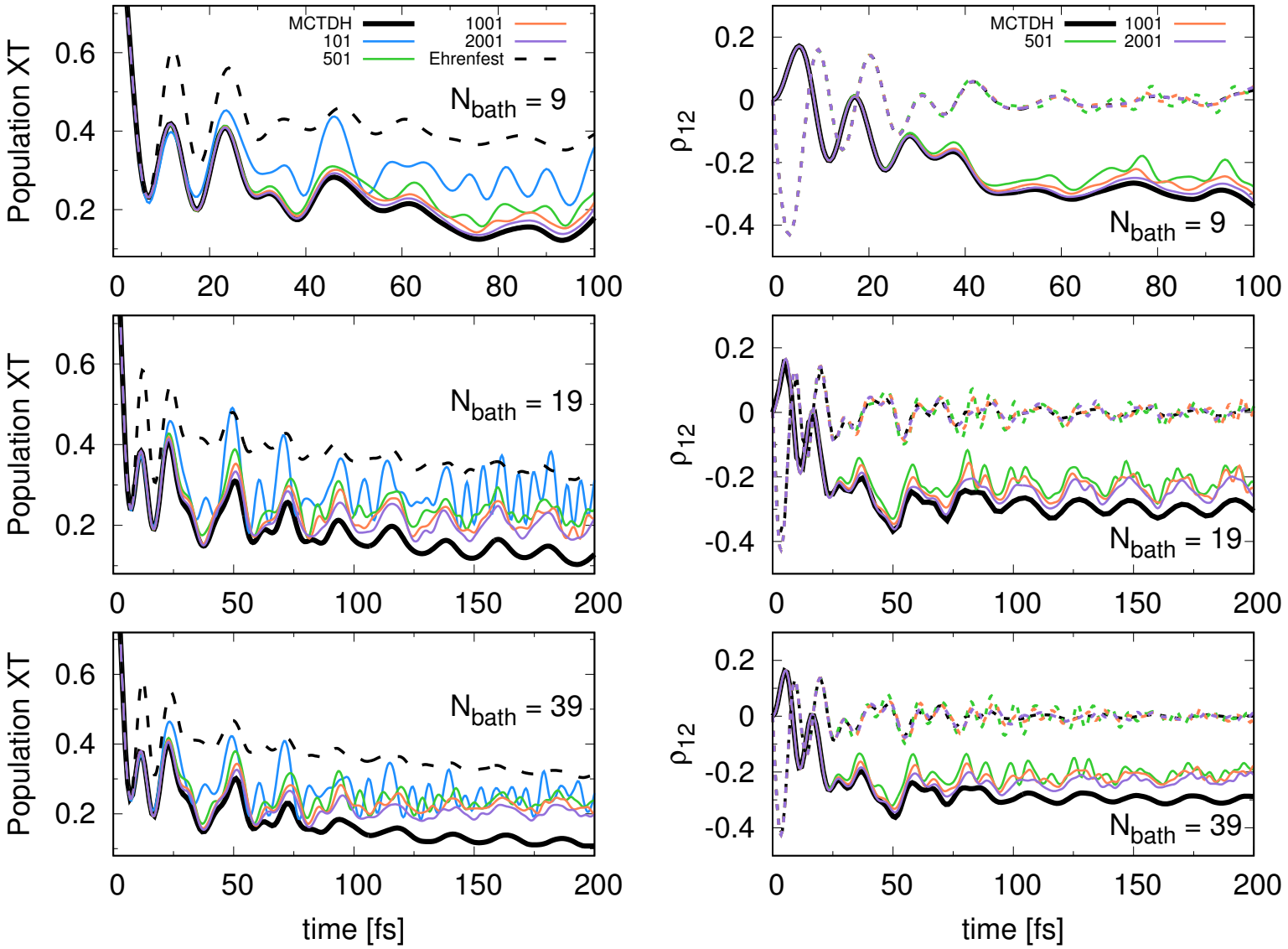

G-MCTDH: System-Bath Models

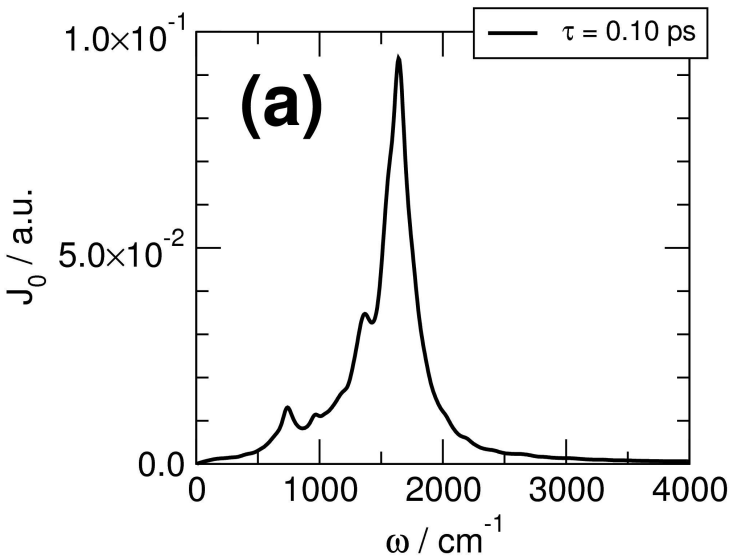

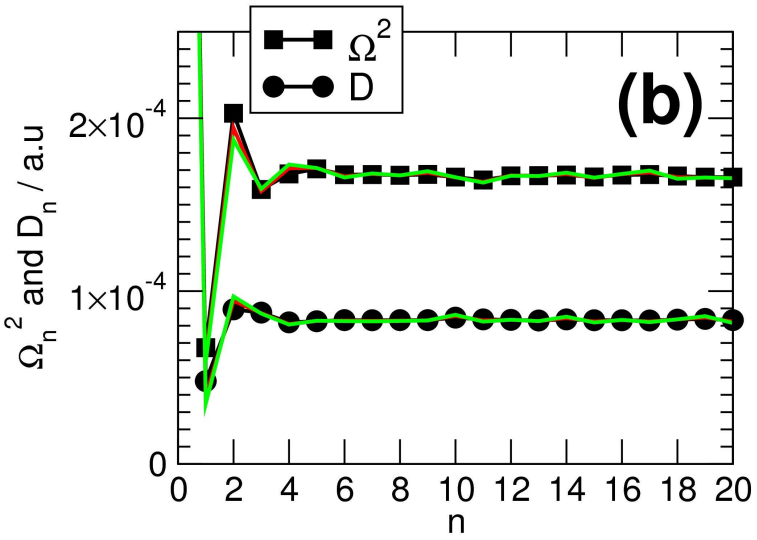

- discretized bath spectral densities (SDs) represented by "GWP bath"
- hierarchical chain representations of SDs that are (partially) represented by GWPs including Langevin closure

$$\hat{H}_{SB} + \hat{H}_B = \hat{s} \sum_i c_n \hat{x}_n + \hat{H}_B \longrightarrow D\hat{s}\hat{X}_1 + D_{12}\hat{X}_1\hat{X}_2 + \ldots + \hat{X}_M\text{–residual bath}$$

Approximate SD's: Mth Order Truncation

$$J(\omega) = \frac{\pi}{2} \sum_n \frac{c_n^2}{\omega_n} \delta(\omega - \omega_n) \quad \longleftrightarrow \quad J^{(M)}(\omega) = \lim_{\varepsilon \to 0^+} \mathrm{Im}\, K_B^{(M)}(\omega - i\varepsilon)$$

Hughes, Christ, Burghardt, JCP 131, 124108 (2009), Garg, Onuchic, Ambegaokar, JCP 83, 4491 (1985), Leggett, Phys. Rev. B 30, 1208 (1984)

$$K_B^{(M)}(z) = -\cfrac{D_{0,1}^2}{\Omega_1^2 - z^2 - \cfrac{D_{1,2}^2}{\Omega_2^2 - z^2 - \cdots \cfrac{D_{M-2,M-1}^2}{\Omega_{M-1}^2 - z^2 - \cfrac{D_{M-1,M}^2}{\Omega_M^2 - z^2 - z^2 I^M(z)}}}}$$

Ohmic closure:

$$I^M_{\mathrm{ohm}}(z) = -i\frac{\gamma}{z}$$

Rubin (quasi-Ohmic) closure:

$$I^M_{\mathrm{Rubin}}(z) = \frac{1}{2z} \frac{{\Lambda_R}^2 - 2z^2 + 2iz\sqrt{{\Lambda_R}^2 - z^2}}{z + i\sqrt{{\Lambda_R}^2 - z^2}}$$

Hughes, Christ, Burghardt, J. Chem. Phys. 131, 024109 (2009), Martinazzo, Vacchini, Hughes, Burghardt, J. Chem. Phys. 134, 011101 (2011)